Siliciclastic sediment volumes and rates of the North Pyrenean Retro-Foreland Basin

Alexandre Ortiz, François Guillocheau, Cécile Robin, Eric Lasseur, Justine Briais, Charlotte Fillon

SILICICLASTIC SEDIMENT VOLUMES AND RATES OF THE NORTH PYRENEAN RETRO-FORELAND BASIN

Alexandre Ortiz[1], François Guillocheau[1], Cécile Robin[1], Eric Lasseur[2], Justine Briais[2], Charlotte Fillon[3]

1: Univ Rennes, CNRS, Géosciences Rennes - UMR 6118, 35000 Rennes, France

2: BRGM (French Geological Survey), 45060 Orléans Cedex 2, France

3: TotalEnergies, Research and Development, 64018 Pau Cedex, France

Corresponding author[1]: Alexandre ORTIZ

Univ Rennes, CNRS, Géosciences Rennes - UMR 6118, 35000 Rennes, France

Email address: alex.ortiz@hotmail.fr

[1] Present-day affiliation : BRGM (French Geological Survey), 45060 Orléans Cedex 2, France

Acknowledgments

This work is part (and supported by) the 'Source-to-Sink compression' project that is jointly managed by TotalEnergies and the French geological survey BRGM. The original manuscript was significantly improved by the editor, Cari Johnson and the contribution of John M Holbrook and anonymous reviewer during the peer-review process.

Abstract

Sediment accumulation rates in foreland basins results from a complex interplay between surface and deep processes in both the exhumed relief domain and sedimentary basins. The growth and decay of a mountain belt during orogenic and post-orogenic phases have been largely studied thanks to thermochronological and structural studies. The sedimentary response of the orogenic phases in the preserved sediments of the surrounding basins is well known in terms of sedimentary filling patterns and architecture, but much less better quantified.

Here, we performed a measurement of the siliciclastic sediment volumes of the Pyrenean retro-foreland basin – the Aquitaine Basin and the Bay of Biscay during Cenozoic times – for a better understanding of the erosion and the sediment transfer and deposition during the convergence (syn-orogenic) to post-convergence (post-orogenic) periods of the Pyrenees Mountain. The measurement of the compacted siliciclastic sediment is based on sediment thickness (isopach) maps of known lithologies, derived from the interpretation of 40 000 kms of seismic profiles.

Thanks to the siliciclastic sediment volumes quantification and a well-known retro-foreland basin tectono-sedimentary evolution, we bring quantitative results as:

(1) The amount of preserved sediments is of 51 500 ± 16 800 km^3 for the Cenozoic.
(2) The siliciclastic sediment rate curve during Cenozoic shows two major increase around 26.0 Ma and 2.5 Ma. The 26.0 Ma increase is clearly related to the erosion of the Pyrenees of tectonic origin. The major 2.5 Ma one would be mainly related to a climatic forcing.
(3) The mass balance between the Aquitaine Platform and the deepest domains change through time in favour of the deep domain. This might be explained by the ratio between subsidence that created accommodation space and the sediments feed by the mountain belt and stored in the Aquitaine Platform.

Keywords: accumulation rates, retro-foreland, Pyrenees, Aquitaine Basin, Bay of Biscay, Cenozoic

1. Introduction

The growth and decay of mountain belts reliefs result from feedbacks between convergence rates, surface processes (Beaumont et al., 1992; Willett, 1999) and isostatic response (Molnar and Lyon-Caen, 1988; Watts, 2001). The topography of a mountain belt is first built by continental crust thickening during convergence, generating loading on the lithosphere and its downward deflection at the origin of the surrounding foreland basins and their vertical motion (Beaumont, 1981; Allen and Allen, 2013). Topographic evolution of the mountain belt is also influenced by climate which can modify the erosion by surface processes (e.g. Whipple, 1999). Finally, the base level variations in the foreland basins may play a dominant role, on piedmont dynamics, in preserving reliefs (base level rise with emplacement of endorheism, Babault et al., 2005) or enhancing its incision (base level fall by major capture for instance, see Burbank and Anderson, 2009)

The estimation of denudation, i.e. the amount of eroded rocks, through time and its controls by lithospheric deformation and/or climate (precipitation) are of primary importance for understanding (1) the topographic growth and decay of mountain belts, but also (2) the volumes and lithologies of the sediments produced and transferred to the surrounding basins. The quantification of the denudation of a mountain belt is mainly based on low temperature chronology (e.g. fission track and (U-Th)/He on apatite and zircons – ZFT, AFT, ZHe, AHe) that provides a cooling history classically converted into exhumation with using thermal numerical models (Braun, 2003 for instance, Ketcham, 2005; Gallagher et al., 2009). The sediment production (volumes, petrography and grain-size) was performed on several foreland basins (Molnar and England, 1990; Einsele, 2000; Najman and Garzanti, 2000; Goodbred and Kuelh, 2000; Schlunegger et al., 2001; Garzanti, 2019). In the Pyrenean domain, the P. Allens's group has carried out numerous studies on these thematic, focus on the southern side (e.g. Michael et al., 2013, 2014 a,b; Armitage et al., 2015).

The quantification of the siliciclastic sediment volume (sink) in foreland basins was first performed at mountain-scale in the Alps (England, 1981, Kuhlemann, 2000; Kuhlemann et al., 2002), but most of them concerns the latest deposition stages found in the ultimate sink: the passive margin laterally connected to the foreland basins. This is the case for Asian mountains (Métivier et al., 1999; Clift et al., 2006) or Rocky Mountains and the margins of the Gulf of Mexico (Galloway and Williams, 1991; Galloway et al., 2011). They all show an increase of the sedimentation rates up to today, a critical point discussed by P. Molnar (Molnar and England, 1990; Molnar, 2004) that might be related to global climate cooling (e.g. Herman and Champagnac, 2016) and/or large erosion/recycling of the foreland deposits (Schlunnegger and Mosar, 2011; Leroux et al., 2017), linked frontal accretion, climate variations and drainage network reorganization. Thus, the volumes distribution (storage, transfer, recycling) between the foreland and the final sink at different stages of mountain belt evolution have not been fully explored since the synthesis of Hinderer, 2012.

We propose in this study to measure the siliciclastic sediment volumes in a retro-foreland basin where limited frontal accretion allows a more complete preservation of syn-tectonic deposits – the Aquitaine Basin and the Bay of Biscay during Cenozoic times for a better understanding of the erosion, the sediment transfer and deposition during the convergence to post-convergence periods of the Pyrenees Mountains and discuss at the first order the tectonic and climatic control factors. The measurement of the compacted siliciclastic sediment volumes (for a solid rocks equivalence) are based on sediment thickness (isopach) maps of known lithologies, built from an extensive dataset of seismic lines interpreted using the principles of seismic stratigraphy and dated on wells (Ortiz et al., 2020).

2. Geological setting

The North Pyrenean retro-foreland and its lateral deep area of ultimate sediment deposition – the deep Bay of Biscay Basin – is segmented into three geographical-geological units (Fig. 1): (1) upstream, bounded westward by the Pamplona transfer zone, the Aquitaine Platform (i.e. the modern onshore Aquitaine Basin and its shelf), (2) the Landes Plateau, bounded westward by the Santander "soft" transfer zone, is a step (1000-1800 m deep) bounded by slopes and canyons (Capbreton, Cap-Ferret) and (3) the deep Bay of Biscay (4000-4500 m deep).

2.1. Tectonic, relief and exhumation evolution of the Pyrenees

The Pyrenees Mountains are a collisional belt bringing Eurasian lithosphere over the Iberian lithosphere (e.g. Roure et al., 1989; Muñoz, 1992). Both Pyrenees and Basque-Cantabrian Mountains result from the inversion and compression of the Albian hyperextended Eurasian lithosphere (e.g. Fabriès et al., 1991, 1998; Lagabrielle et Bodinier, 2008; Jammes et al., 2009; Lagabrielle et al., 2010; Masini et al., 2014; Clerc et al., 2012, 2016; Ducoux et al., 2019; Saspiturry et al., 2019; Ducoux et al., 2021, Tugend et al., 2014). The relative motion of Eurasia and Africa plates controlled the orogeny: the compression started at the time of convergence of the two plates, i.e. at the end of the Santonian (83.6 Ma, Schettino and Turco, 2011) and ended around the Oligocene-Miocene boundary (chron 6c, Roest and Srivastava, 1991, Macchiavelli et al., 2017).

Thermochronological data also document the early mountain building with a cooling phase at around 70 Ma (Whitchurch et al., 2011; Beamud et al., 2011; Mouthereau et al., 2014; Ternois et al., 2019; Waldner et al., 2021). During Cenozoic, several studies resolve the increase of exhumation during late Eocene-Oligocene times (Fitzgerald et al., 1999; Sinclair et al., 2005; Gibson et al., 2007; Jolivet et al., 2007; Gunnel et al., 2009; Metcalf et al., 2009; Whitchurch et al., 2011; Fillon and van der Beek, 2012; Bosch et al., 2016) following an earlier uplift of the eastern range during Middle Eocene times (Maurel et al., 2008; Beamud et al., 2011; Mouthereau et al., 2014; Vacherat et al., 2014; 2016; Ternois et al., 2019; Whitchurch et al., 2011; Waldner et al., 2021). Finally, a late Miocene exhumation phase is recorded in the Western Pyrenean Range by several authors (Jolivet et al., 2007; Bosch et al., 2016; Fillon et al., 2021)

2.2. Stratigraphic and tectonic evolution of the Aquitaine Basin and Bay of Biscay deep Basin

Several studies have been carried out on the tectono-stratigraphic evolution of the Aquitaine Basin since the late Cretaceous (Brunet, 1984; Desegaulx and Brunet, 1990; Brunet, 1994; Sztrákos et al., 1998; Serrano et al., 2001; Ford et al., 2016; Sztrákos and Steurbaut, 2017; Angrand et al., 2018). They identified two subsiding phases (Latest Santonian - Danian and Thanetian – Oligocene) separated by the so called “Palaeocene quiet period” characterized by a low to near zero subsidence phase (Ford et al., 2016). The first subsidence phase has been largely influenced by the post rift thermal subsidence because of the short time between the end of the rifting and the beginning of the convergence (around 10 Ma, Angrand et al., 2018). Serrano et al., (2001) differentiate two distinct phases in the Western Aquitaine Basin (1) from Palaeocene to Middle Eocene - compressional basin due to lithospheric buckling (mixed system – East-West oriented turbidites and carbonates platform) and (2) from Middle Eocene to Oligocene – foreland stage (progressive continentalization on the eastern part and deltaic progradation toward the West).

Recently, through an extensive bio- and seismic stratigraphy study of both basins, Ortiz et al. (2020) identified a set of several discontinuities of tectonic origins (fig. 2). The orogenic period is subdivided into two steps (fig. 2): (1) the dominant lithosphere flexure with the formation of foredeeps up to the uppermost Lutetian and (2) the propagation of the deformation from the orogenic wedge through the basin mainly along salt-controlled thrusts and anticlines locating subbasins. From the basin record point of view, the transition between orogenic and post-orogenic periods is Chattian in age, from 27.1 to 25.2 Ma. This time interval corresponds to the end of thrusting/inversions and a modification of the sediment preservation pattern. The post-orogenic period is also subdivided into two intervals (fig. 2): (1) a sharp decrease of the subsidence rates over the Aquitaine Platform, mainly filled by continental sediments during early Miocene times (25.2-16.4 Ma) and (2) an uplift of the Aquitaine Platform from 16.4 Ma to today characterized by a low-preservation domain up to 10.6 Ma. The main uplift phase occurred at 10.6 Ma and caused a generalized by-pass on the Aquitaine Platform (Ortiz et al., 2020).

3. Measurement of siliciclastic sediment volumes and rates

The measurement of siliciclastic sediment (sink) volumes is based on four sediment thickness (isopach of preserved sediments) maps: Palaeocene-Eocene (66-33.9 Ma - fig. 3), Oligocene (33.9-23.03 Ma - fig. 4), Miocene (23.03-5.3 Ma - fig. 5) and Pliocene-Pleistocene (5.3-0 Ma - fig. 6). These isopach maps are the products of a seismic stratigraphic analysis of an extensive seismic line dataset (TotalEnergies, BRGM, BSS, fig. 1). This quite low time-resolution is due to the absence of wells in the deep Bay of Biscay and the difficulty to extend timelines from the Aquitaine Platform where several dated wells are available (see Ortiz et al., 2020). For each interval the main lithologies proportion is known in the Aquitaine platform and in the Landes Plateau (see Ortiz et al., 2020) and for the distal part of the Bay of Biscay, we used the studies available in this domain about the Cenozoic sedimentary record (Cremer, 1983; Iglesias, 2009; Brocheray et al., 2014).

The sediment volumes measured from the isopach maps were later decompacted and the amount of sediments produced in the basin (here mainly carbonates) was removed to get solid rock volumes. We used the protocol and code published by Guillocheau et al. (2012) that consider uncertainties or ranges for (1) time-depth conversion parameters, (2) absolute ages of the different horizons, (3) carbonate content and (4) surface porosity and e-folding depth for porosity decrease. During Cenozoic times the deep-sea Bay of Biscay fan fed through the Capbreton and Cap-Ferret Canyon by the sediments coming from the Aquitaine Basin has progressively migrated westward (Cremer, 1983; Iglesias, 2009; Brocheray et al., 2014), our calculation area is evolving accordingly (dashed line on figs, 3, 4, 5, 6). In order to compare the volumes, they will be presented through the evolution of the ratio between Aquitaine Basin volume (V_{On}) and Bay of Biscay volume (V_{Off}) as follow: $R_{OnOff} = V_{On}/V_{Off}$.

4. Isopach maps: results and interpretation

4.1. Paleocene-Eocene (66-33.9 Ma)

The *Paleocene-Eocene* (66-33.9 Ma - Fig. 3) time interval is characterized by sediment preservation along the North Pyrenean Thrust on the Aquitaine Platform, with three subsiding domains - 10-50 km large - filled by 3500 m of sediments accumulated in 32 Ma. Two less subsiding domains were located north of the previous ones and bounded by two ridges with very low accumulation. Few sediments were preserved along the Landes Plateau. In the deep Bay of Biscay, two depocenters occurred south of the South Armorican Margin and north of the Biscay Wedge Front.

Interpretation: The three subsiding domains correspond to a segmented foredeep (Ortiz et al., 2020) controlled by the inherited structures from the Early Cretaceous rifts history (Angrand et al., 2018). These domains are mainly filled during the first orogenic phase (up to uppermost Lutetian) and the small depocenter in the northern part of the ridges correspond mainly to the second orogenic phase, when the deformation is propagated basinward. The two deep depocenters of the Bay of Biscay are disconnected from the Aquitaine Platform and bounded by the inverted extensional structures of the Gascogne Dome Bulge (Thinon, 1999; Thinon et al., 2001). The first depocenter located in the Armorican subbasin, was fed by sediments coming from the Loire River (fig. 1) or from the Armorican Massif (Guillocheau et al., 2003).

4.2. Oligocene (33.9-23.03 Ma)

The *Oligocene* (33.9-23.03 Ma - fig. 4) was a period of more widely distributed sediments accumulation along the three domains. In the Aquitaine Platform depocenters are located (i) on both sides of salt-related controlled thrusts forming anticlines or ridges (Maubourguet-Antin, Audignon) or (ii) along N140° faults (e.g. Téthieu Fault, location on figures 1 and 4). In the south Landes Plateau, north of the Basque-Cantabrian Mountains, a 60 km-large depocenters occurred. In the deep Bay of Biscay, a NW-SE trending depocenter is located south-west of the inverted structures of the Gascogne Dome Bulge and north of the Biscay Wedge Front.

Interpretation: Oligocene is a period during which (1) segmented foredeep was no longer subsident and (2) compressive deformation propagated from the orogenic wedge to the retro-foreland basin along salt decollement levels localizing little subbasins (Serrano, 2001; Ortiz et al., 2020). The depocenters of the south Landes Plateau may be due to the loading effect of the inverted and thrusted Basque Cantabrian Margin starting at 37 Ma and ending at 28.5 Ma (Gomez et al., 2002). The depocenter of the deep Bay of Biscay is disconnected from the Aquitaine Platform and moderately fed by the erosional product coming from the inversion and deformation of the Cantabrian Margin and the uplift of the Cantabrian Mountains from Late Eocene to Oligocene times (Gallastegui et al., 2002; Pedreira et al., 2015; Fillon et al., 2016).

4.3. Miocene (23.03-5.3 Ma)

The *Miocene* (23.03 to 5.3 Ma – fig. 5) recorded a major change in the sediment distribution. The Aquitaine platform was henceforth a place of low sediment preservation (less than 200 m for 17.5 Ma). Most of the sediments were transferred and stored along the

Landes Plateau and the deep Bay of Biscay. Two major sediment accumulations were active in the Landes Plateau, (1) to the north, a progradational wedge (Ortiz et al., 2020) located at the transition between the southeastern part of the South Armorican shelf and the Landes High and (2) to the south, an E-W trending depocenter located north of the Capbreton canyon. The preserved sediments along the deep Bay of Biscay are organized as an E-W trending body more than 100 km-large located on the Biscay Wedge Front. It is upstream in connection with the two depocenters of the Landes Plateau.

Interpretation: The Aquitaine Platform was no longer a significant subsiding domain. Most of the sediments bypassed to deepest areas: (1) through deltaic progradational wedges on the Landes Plateau, (2) through canyons and at the end of the system (3) as deep-sea fans. The depocenters located north to the Capbreton canyon correspond to the northern levee of the canyon already active at this period (Cremer, 1983; Iglesias, 2009, Ortiz et al., 2020). Progradationnal deltaic wedge accumulate at the head of the Cap-Ferret canyon (western extension of the north Landes Plateau depocenter – Cremer, 1983) and downstream (East of the deep Bay of Biscay depocenter), an erosion domain where the canyon is active. These two canyons domains fed downward, the Cap-Ferret deep-sea fan (Cremer, 1983; Iglesias, 2009) in the deep Bay of Biscay.

4.4. Plio-Pleistocene (5.3-0 Ma)

The *Pliocene-Pleistocene* (5.3-0 Ma – fig. 6) time-interval shows an accentuation of the sediment distribution pattern established during Miocene. (1) No to very few sediments were preserved on the Aquitaine Platform. (2) Two depocenters occurred on the Landes Plateau: (i) a N-S trending one north to the Landes High (progradationnal wedges – Ortiz et al., 2020) and

(ii) a N-S trending one south of the Landes High. (3) The depocenters of the deep Bay of Biscay are located (i) at the base of slope of the South Armorican shelf and (ii) along the Biscay Wedge Front in connection with the northern depocenter of the Landes Plateau.

Interpretation: The Aquitaine Plateau was upstream uplifted and incised by rivers (Mouchené et al., 2017; Ortiz et al., 2020). All the products of erosion are transferred to the deepest domains with by-pass to very low sedimentation along the modern Landes Forest (Dubreuilh et al., 1995). The prograding sedimentary wedge is now located at the border of the Aquitaine shelf and the two canyons (Capbreton and Cap-Ferret) alternated periods of erosion and deposition (Cremer, 1983; Iglesias, 2009).

5. Measurement of the siliciclastic sediment budget: results (fig. 7)

In the deep-sea plain, siliciclastic volume measurements were only performed in the south deep Bay of Biscay Basin, south of the Gascogne Dome Bulge, the sediment located northward (Armorican Subbasin) being fed from the Loire River (fig. 1) and the Armorican Massif (see 4.1). In addition, during Cenozoic times the deep-sea Bay of Biscay fan fed through the Capbreton and Cap-Ferret Canyon by the sediments coming from the Aquitaine Basin is progressively migrating westward (Cremer, 1983; Iglesias, 2009; Brocheray et al., 2014). This is the reason why, our calculation area is evolving according to the deep-sea fan location (Figs, 3, 4, 5, 6).

The total amount of siliciclastic sediments (Tab. 1, Fig. 7) deposited from the Aquitaine Platform to the south deep Bay of Biscay during Cenozoic times is 51 500 km^3 with an uncertainty of 16 800 km^3, i.e. 33%.

The four-time intervals here defined, have not the same duration and therefore siliciclastic sedimentation rates had to be used for a comparison between time intervals instead of volumes (Tab. 1, fig. 7). At first order the sedimentation rates are increasing from 535 km^3/Myr (between 66 and 33.9 Ma) to 3150 km^3/Myr (from 5.3 to 0 Ma). Oligocene and Pliocene-Pleistocene seems to be significant instants of siliciclastic sediment rates increase.

The siliciclastic sediment budget comparison (Tab. 1, fig. 7) between the onshore (Aquitaine Basin) and offshore (Aquitaine shelf, Landes Plateau, south Bay of Biscay) shows a shift, trough Cenozoic times, from onshore to offshore preferential accumulation since Oligocene-Miocene boundary. The sediment ratio between onshore and offshore (R_{OnOff}) is (i) 25.3 from 66 to 33.9 Ma, (ii) 7.5 from 33.9 to 23.03 Ma, (iii) 0.18 from 23.03 to 5.3 Ma and (iv) 0.01 from 5.3 to 0 Ma.

6. Discussion on the siliciclastic sediment budget

Volume comparison with South Pyrenean Foreland and others orogenic adjacent basins - The amount of siliciclastic sediments preserved in northern foreland is 51 500 ± 16 800 km^3 for Cenozoic times. A comparison with the sediment volumes of other orogenic systems supposes to get a sediment budget for both sides of the Pyrenees, i.e. including the South Pyrenean Foreland basin. Several studies have been conducted for quantifying the preserved sediment volumes in the South Pyrenean sink (i.e. Ebro and Valencia Basins)(Nelson, 1990; Garcia-Castellanos et al., 2003; Babault et al., 2006; Filleaudeau, 2011; Arche et al., 2010; Watts and Torné, 1992). The Ebro Basin has been under endoreic conditions since 36.2 Ma

(Costa et al., 2010) and then opened towards the Mediterranean Sea between 12 Ma and 7.5 Ma (Garcia-Castellanos et al., 2003; Fillon et al., 2012; Garcia-Castellanos and Larrasoana, 2015). The total amount of preserved sediments in the Ebro and Valencia Basin is 260 300 km^3 since 66 Myr. For a better sediment budget on both sides of the Pyrenees, only the sediments coming from the mountain belt should be considered, i.e. the total Cenozoic preserved sediments volumes in the Ebro basin and the Neogene for the Valencia Basin. This corresponds to a range between 78 000 km^3 (Filleaudeau, 2011) and 110 000 km^3 ± 5000 km^3 (Garcia-Castellanos et al., 2003) in the Ebro Basin and 92 000 km^3 in the Valencia Basin (Garcia-Castellanos et al., 2003). This gives a total of preserved sediments between 170 000 km^3 and 202 000 km^3. At the first order, this result shows a factor of four between the northern retroforeland (our study) and the South Pyrenean proforeland.

The first-order estimation of total volume preserved in the Pyrenean adjacent basins (i.e. Aquitaine Basin, Bay of Biscay, Ebro Basin, Valencia Basin) is between 220 000 km^3 and 250 000 km^3. The total volume of siliciclastic sediments produced by the Alps since Oligocene times is of 890 000 km^3 (220 000 km^3 from the Eastern Alps and 670 000 km^3 from the western ones- Kuhlemann et al., 2002) i.e. four times more than the Pyrenees. However, for larger orogens the order of magnitude changes with 3.35 10^6 km^3 of sediment produced by the Rocky Mountains on its continental part and stored in the Gulf of Mexico (Galloway et al., 2011) and the 4.95 10^6 km^3 by the western side of the Himalaya and accumulated along of the Indus Delta (Clift et al., 2006).

Volume comparison with Pyrenean thermochronological data – We present here some volumes estimation for the Cenozoic period based on published themrochronology data in the Pyrenees.

- Too few data (AFT and AHe) provide Palaeocene to early Eocene ages to obtain a consistent exhumation trend across the entire Pyrenean range.

- During the late Eocene/lower Oligocene (from 37 to 30 Ma), orogenic exhumation (> 0.5 km/Myr) is recorded in Central and Eastern Pyrenean Massif (Maladetta, Nogueres, Canigou) according to studies from Fitzgerald et al., (1999), Gibson et al., (2007), Fillon and Van der Beek, (2012) and Gunnel et al., (2009). These authors modeled an exhumation rate of 1.5 to 4 km/Myr. Considering an average of 2 km/Myr integrated over the whole area (inducing a strong assumption of a continuous constant exhumation) during the period of 35-30 Ma, the eroded volume should be of 50 000 km^3. This value is very high compared to what has been measured in the Aquitaine Basin during the same period (16 500 km^3 from base Cenozoic to base Oligocene). This volume seems therefore to supply mainly the Ebro basin with a significant increase observed at the base of Oligocene (i.e. 33.9 Ma) (Filleaudeau, 2011).

- Since middle Oligocene times, a moderate exhumation (between 0.1 and 0.5 km/Myr) is proposed by several authors in Western, Central and Eastern massifs of the Pyrenean range (DeFelipe et al., 2019; Bosch et al., 2016; Fillon et al., 2021; Fitzgerald et al., 1999; Gibson et al., 2007). An average exhumation rate of 0.25 km/Myr across the entire range provides an estimation of 17 500 km^3 for the Middle to Late Oligocene period. This volume is, like during Late Eocene/Lower Oligocene, one order of magnitude higher than what we measure in the Aquitaine Basin. This volume supply mainly the Ebro basin where the Oligocene volumes are very large (around 45 000 km^3 in Filleaudeau, 2011).

- Finally, the important increase of exhumation rate recorded in the Western Pyrenees (see Fillon et al., (2021) for the data synthesis and modelling) infers a volume estimation of 2 000 km^3 for the late Miocene period. This quantification is low compared to the volumes of preserved sediments.

We draw attention to the fact that these estimation are produces from an average of the results of modelling data done in 1D and extrapolated on a surface. These volumes based on thermochronological data are probably overestimated.

6.1. Age estimation of siliciclastic sediment flux increase from interpreted seismic data

As we mentioned earlier, the low stratigraphic resolution (Palaeocene-Eocene, Oligocene, Miocene and Pliocene-Pleistocene) is due to difficulties to propagate the high resolution age model (established in shallow marine setting in the Aquitaine Platform and Landes Plateau – Ortiz et al., 2020) across the whole seismic survey in the deep Bay of Biscay Basin and continental Aquitaine series. In order to be more precise about the age of the siliciclastic rate increase during the two key periods (Oligocene and Plio-Pleistocene) and their possible links to climatic or geodynamic event, we performed a 2D quantification on the cross section published in Ortiz et al., (2020). This quantification aims at comparing on three different locations (proximal Aquitaine platform – deep Bay of Biscay Basin – progradational wedges in between) the percentage of 2D surface (comprising sediment) normalized on their duration between each high-resolution timeline.

The figure 8 present the results and shows a refined estimate of increase at 26.0 ± 2.0 Ma for Oligocene period and 2.5 ± 0.5 Ma for Pliocene-Pleistocene period.

6.2. The 26.0 ± 2.0 Ma increase

The measured Late Oligocene (26.0 ± 2.0 Ma) siliciclastic rate increase could be explained by both a tectonic factor – the accretion of Pyrenees basal units – and a climatic factor – the icehouse-greenhouse transition and the late Oligocene warming (Zachos et al., 2001).

Tectonic - A Late Eocene to Oligocene/Miocene paroxysm of denudation (37-29 Ma central Pyrenees and 37-20 Ma western Axial Zone) is measured by the numerous thermochronological studies (see references in section 2.1) and by the dated active tectonics mainly in the Southern Pyrenees (Montsec and Sierras exteriores thrust systems associated to Orri and Rialp thrust sheets, see Munoz, 1992, Teixell, 1998, Vergés et al., 2002 and Mouthereau et al., 2014), or in the Jaca Basin cover thrust and associated Gavarnie and more frontal thrusts (Labaume et al., 2016). During late Oligocene time, the retro-foreland is affected by several truncation/erosional surfaces from 27.1 to 25.2 Ma (Ortiz et al., 2020). During this event, some syn-orogenic deposits are recycled and can be transferred to more distal sink. The observed increasing volumes and increasing export of sediment to the Bay of Biscay is thus contemporaneous with a (long) denudation paroxysm, but also with a more temporally resolved drop of preservation in the foreland which becomes less subsident and might be locally eroded and recycled. The observed modification of source to sink pattern might record combination of two processes, denudation increasing phase and cessation of subsidence in the foreland could explain the increase export toward the final sink and sedimentation rate increase observed in the western Aquitaine Platform part (fig. 4).

Climate - Few palaeoclimatological data dealing with the palaeoprecipitation record are available in the Aquitaine Basin. A palaeobotanical synthesis (Dupéron-Laudoueneix and Pons, 1985) indicate a cooling expressed by a decrease of the tropical taxon from the Eocene to the Oligocene that corresponds to the Eocene-Oligocene global cooling event (Zachos et al., 2011). This event takes place at 33.9 Ma, thus well before the observed 26 Ma event.

The 26.0 ± 2.0 Ma increase event is contemporary with the Late Oligocene Warming, that correspond to a sustained *ca.* 6°C global warming (Zachos et al., 2001). Warming events (such as PETM) can cause sediment pulses (Foreman et al., 2012). Schlunegger and Norton, (2015) have tested this increase hypothesis in the Alpine Foreland Basin. They focus on the Napf megafan sedimentary evolution in the Alpine foothills during this period of sudden warming. As in our study the period is also a time of increasing exhumation phase in the Alpine mountain (Schmid et al., 1996). They didn't observe remarkable shift in the water discharge, and they ruled out the hypothesis of sediment rate increase due to the Late Oligocene warming but linked it to tectonic process.

In our case, the Late Oligocene (26.0 ± 2.0 Ma) siliciclastic rate increase is linked to the high erosion rates and lower preservation in the Aquitaine Platform controlled by the orogenic tectonic processes. This increase is also registered in the Ebro basin (Filleaudeau, 2011).

6.3. The 2.5 ± 0.5 Ma increase and the long-term volume increase

The change in the rate of siliciclastic sediment supply during Plio-Pleistocene (at 2.5 ± 0.5 Ma) is significant (fig. 8) and sharply accentuates the overall increasing rate trend through Cenozoic times. This confirms for this area, the Hay's curve (Hay et al., 1989, 1990; Wold et Hay, 1990) showing a world-scale increase of the siliciclastic fluxes up to today, interpreted by Molnar (Molnar and England, 1990; Molnar, 2004) as the consequence of the global Earth cooling during Plio-Pleistocene times. Herman et al., (2013) further suggest a Plio-Pleistocene (at around 6 Ma) increase in erosion rates and with an acceleration at around 2 Ma that they attribute to the global cooling Pliocene and Pleistocene episodes that enhanced erosion in mountainous glaciated area.

Onshore, the most sensible low-temperature thermochronological data, ((U-TH)/He and Fission tracks on apatites) do not show any Pliocene increase of denudation either in the Pyrenees Mountains (e.g. Bosch et al., 2016) or in the French Massif central (T. François, personal communications). The youngest cooling episode is recorded at around 10 Ma (Late Miocene) in the western axial zone and no basin erosion > 1.5 km could be retrieved in the Aquitaine Basin for the last 20 Myrs (Fillon et al., 2021), except in easternmost Aquitaine Basin (Corbières area) Al Reda et al., (2021) althought this denudation event is temporally poorly resolved between 20 and 5 Ma, this event is attributed by the authors to early Miocene and opening of the Gulf o Lion.

With these observations, several hypothesis have yet to be tested: (1) a climate effect on the intensity and pattern of erosion, with the effect of glaciations and change of the pattern of erosion, from widely distributed before 5.3 Ma to localized in valleys after with a greater climate effect from 2 Ma, which could be associated to (2) an “underestimated” significant re-erosion of previously deposited sediments in the Aquitaine Basin (“cannibalization”) and (3) lateral supply of sediments from other sources in the deep-sea domain under the action of deep-sea currents (Le Danois Contourite Depositional System due to Mediterranean Outflow Water, Van Rooij et al., 2010). Moreover, Pliocene-Pleistocene evolution of the Aquitaine Platform records a two steps evolution, the emplacement of megafans with the most striking one i.e. Lannemezan megafan starting during Messinian up to Uppermost Pliocene (Ortiz et al., 2020). This megafan mainly source by the Neste River is dissected during Late Quaternary (at or before 300 ka, Mouchené et al., 2017). This indicates a shift from a sedimentation phase to an incision phase, that takes place between 2.6 Ma and 300 ka. This supports the hypothesis of recycling by erosion of previous deposits sediments in the Aquitaine Platform.

Although glaciations is well documented during Late Quaternary in the Pyrenees (Calvet et al., 2011; Delmas et al., 2008), their importance in terms of sedimentary budget is still not quantified. Identified glacial remnants are restricted to the upper part of the valleys and mostly confined in the mountains belts (Delmas et al., 2011). The preservation over large areas of preglacial flat surfaces in the high chain (Bosch et al., 2016) claim for erosion localized mainly in glacial valleys. This supports the hypothesis of a more localized erosion in the mountain valleys.

6.4. Sediment budget evolution between onshore and offshore

The change of the sediment ratio between onshore and offshore (R_{OnOff}) from 25.3 (66 to 33.9 Ma) to 0.01 (5.3 to 0 Ma) has to be related to the general evolution of the two basins as summarized in item 2.2. This drastic change of ratio in favour of the “ultimate sink” is in line with the synthesis of Hinderer, 2012.

- The first interval (66.0-33.9 Ma) spans a long period of time and several steps of the orogeny. A first phase (66-56 Ma) of relatively quiescent with very low relief in the mountain belt and siliciclastic input, a second phase (56-33.9 Ma) that correspond to progressive mountain building with increasing relief and erosion. At around 40 Ma, deformation propagate in the foredeep and segmented the foredeep. During this entire period, accommodation space created by the flexure was large enough to trap siliciclastic sediments coming from the incipient mountain belt. This may explain the general trend between 66 and 33.9 Ma.

- The second period (33.9-23.03 Ma) also spans different periods, paroxysm of denudation in the Mountain belt, while in the Aquitaine Platform, two periods are deciphered, a first period of accumulation and deformation (up to 25.2 Ma) and a second with a decrease of subsidence and increase of export to the distal sink (since 25.2 Ma). As a consequence, since 25.2 Ma, siliciclastic supply is too important compare to the accommodation space creation and the sediments are transferred to the progradational wedges in the Aquitaine platform. This explains the trend during Oligocene and particularly since 25.2.
- During the post-orogenic period, first the Aquitaine platform subsidence drastically decreased (25.2-10.6 Ma) and second this domain was partly uplifted (10.6-0 Ma). This favored the sediment export to the deep-sea domain, first poorly balanced (R_{OnOff} at 0.18 – map 23.03-5.3 Ma) and then unbalanced (R_{OnOff} at 0.01 - map 5.3-0 Ma).

7. Conclusion

Our objective was to measure the siliciclastic sediment volumes and rates of a retro-foreland basin and its lateral deep equivalent, during the end tectonic and topographic evolution of the Pyrenees mountain belt.

(1) The amount of sediments is of 51 500 ± 16 800 km^3 for the Cenozoic.

(2) The siliciclastic sediment rate curve during Cenozoic shows two major increase around 26.0 and 2.5 Ma. This last one is a major increase. This is in agreement with the world-scale trend of Hay et al. (1989), expected of climatic origin by Molnar and England (1990).

The 26.0 Ma increase is clearly related to the exhumation of the Pyrenees of tectonic origin. The discussion on the major 2.5 Ma episode is still open.

(3) The mass balance between the Aquitaine Platform and the deepest domains (Landes Plateau, Bay of Biscay) change through time in favour to the deep domain. This might be explained by the ratio between subsidence created accommodation space and the produced siliciclastic sediments by the mountain belt on the platform. This confirms and quantifies the stratigraphic model of sink preservation proposed by Ortiz et al. (2020). This also suggests the sediment accumulation in the deep part of the margin is only controlled by the accommodation/sedimentation balance on the platform.

Data Availability Statement

Research data are not shared

References

Allen, P.A., Allen, J.R., 2013. Basin analysis: Principles and application to petroleum play assessment. John Wiley & Sons.

Al Reda, S. M., Barbarand, J., Gautheron, C., Lasseur, E., Loget, N., Pinna-Jamme, R., & Briais, J., 2021. Thermal record of the building of an orogen in the retro-foreland basin: Insight from basement and detrital thermochronology in the eastern Pyrenees and the north Pyrenean basin (France). *Basin Research*, **33**(5), 2763-2791.

Angrand, P., Ford, M., Watts, A.B., 2018. Lateral variations in foreland flexure of a rifted continental margin: The Aquitaine Basin (SW France). *Tectonics* **37**, 430–449.

Arche, A., Evans, G., & Clavell, E., 2013. Some considerations on the initiation of the present SE Ebro river drainage system: Post-or pre-Messinian?. *Ene*, **13**, 10.

Armitage, J.J., Allen, P.A., Burgess, P.M., Hampson, G.J., Whittaker, A.C., Duller, R.A., Michael, N.A., 2015. Sediment transport model for the Eocene Escanilla sediment-routing system: Implications for the uniqueness of sequence stratigraphic architectures. *J. Sediment. Res.* **85**, 1510–1524.

Babault, J., Loget, N., Van Den Driessche, J., Castelltort, S., Bonnet, S., & Davy, P., 2006. Did the Ebro basin connect to the Mediterranean before the Messinian salinity crisis?. *Geomorphology*, **81**(1-2), 155-165.

Babault, J., Van Den Driessche, J., Bonnet, S., Castelltort, S., & Crave, A., 2005. Origin of the highly elevated Pyrenean peneplain. *Tectonics*, **24**(2).

Beamud, E., Muñoz, J. A., Fitzgerald, P. G., Baldwin, S. L., Garcés, M., Cabrera, L., & Metcalf, J. R., 2011. Magnetostratigraphy and detrital apatite fission track thermochronology in syntectonic conglomerates: constraints on the exhumation of the South-Central Pyrenees. *Basin Research*, **23**(3), 309-331.

Beaumont, C., 1981. Foreland basins. *Geophys. J. Int.* **65**, 291–329.

Beaumont, C., Fullsack, P., Hamilton, J., 1992. Erosional control of active compressional orogens. In: McClay, K. (Ed.), Thrust Tectonics. *Chapman & Hall, London, UK*, pp.1–18.

Bosch, G. V, Teixell, A., Jolivet, M., Labaume, P., Stockli, D., Domènech, M., Monié, P., 2016. Timing of Eocene--Miocene thrust activity in the Western Axial Zone and Chainons Béarnais (west-central Pyrenees) revealed by multi-method thermochronology. *Comptes Rendus Geosci.* **348**, 246–256.

Bosch, G. V., Van Den Driessche, J., Babault, J., Robert, A., Carballo, A., Le Carlier, C., ... & Baudin, T., 2016. Peneplanation and lithosphere dynamics in the Pyrenees. *Comptes Rendus Géoscience*, **348**(3-4), 194-202.

Braun, J., 2003. Pecube: A new finite-element code to solve the 3D heat transport equation including the effects of a time-varying, finite amplitude surface topography. *Computers & Geosciences*, **29**(6), 787-794.

Braun, J., Van Der Beek, P., Valla, P., Robert, X., Herman, F., Glotzbach, C., ... & Prigent, C., 2012. Quantifying rates of landscape evolution and tectonic processes by thermochronology and numerical modeling of crustal heat transport using PECUBE. *Tectonophysics*, **524**, 1-28.

Brocheray, S., Cremer, M., Zaragosi, S., Schmidt, S., Eynaud, F., Rossignol, L., & Gillet, H. 2014. 2000 years of frequent turbidite activity in the Capbreton Canyon (Bay of Biscay). *Marine Geology*, **347**, 136-152.

Brunet, M. F., 1984. Subsidence history of the Aquitaine basin determined from subsidence curves. *Geological Magazine*, **121**(5), 421-428.

Brunet, M. F., 1994. Subsidence in the Parentis Basin (Aquitaine, France): Implications of the thermal evolution. In *Hydrocarbon and petroleum geology of France* (pp. 187-198). Springer, Berlin, Heidelberg.

Burbank, D. W., & Anderson, R. S., 2009. *Tectonic geomorphology*. John Wiley & Sons.

Calvet, M., Delmas, M., Gunnell, Y., Braucher, R., & Bourlès, D., 2011. Recent advances in research on Quaternary glaciations in the Pyrenees. *Developments in Quaternary Sciences*, **15**, 127-139.

Clerc, C., Lagabrielle, Y., Labaume, P., Ringenbach, J.-C., Vauchez, A., Nalpas, T., Bousquet, R., Ballard, J.-F., Lahfid, A., Fourcade, S., 2016. Basement--Cover decoupling and progressive exhumation of metamorphic sediments at hot rifted margin. Insights from the Northeastern Pyrenean analog. *Tectonophysics* **686**, 82–97.

Clerc, C., Lagabrielle, Y., Neumaier, M., Reynaud, J. Y., & de Saint Blanquat, M., 2012. Exhumation of subcontinental mantle rocks: evidence from ultramafic-bearing clastic deposits nearby the Lherz peridotite body, French Pyrenees. *Bulletin de la Société géologique de France*, **183**(5), 443-459.

Clift, P.D., 2006. Controls on the erosion of Cenozoic Asia and the flux of clastic sediment to the ocean. *Earth Planet. Sci. Lett.* **241**, 571–580.

Costa, E., Garces, M., López-Blanco, M., Beamud, E., Gómez-Paccard, M., & Larrasoaña, J. C., 2010. Closing and continentalization of the South Pyrenean foreland basin (NE Spain): magnetochronological constraints. *Basin Research*, **22(6)**, 904-917.

Cremer, M., 1983. Approches sédimentologique et géophysique des accumulations turbiditiques: l'éventail profond du Cap-Ferret (Golfe de Gascogne), la série des grès d'Annot (Alpes-de-Haute-Provence) 1 Thèse, Université de Bordeaux

DeFelipe, I., Pedreira, D., Pulgar, J. A., Van der Beek, P. A., Bernet, M., & Pik, R., 2019. Unraveling the Mesozoic and Cenozoic tectonothermal evolution of the eastern Basque-Cantabrian zone–western Pyrenees by low-temperature thermochronology. *Tectonics*, **38(9)**, 3436-3461.

Delmas, M., Gunnell, Y., Braucher, R., Calvet, M., & Bourlès, D., 2008. Exposure age chronology of the last glaciation in the eastern Pyrenees. *Quaternary Research*, **69**(2), 231-241.

Delmas, M., Calvet, M., Gunnell, Y., Braucher, R., & Bourlès, D., 2011. Palaeogeography and 10Be exposure-age chronology of Middle and Late Pleistocene glacier systems in the northern Pyrenees: implications for reconstructing regional palaeoclimates. *Palaeogeography, Palaeoclimatology, Palaeoecology*, **305**(1-4), 109-122.

Desegaulx, P. A. S. C. A. L., & Brunet, M. F., 1990. Tectonic subsidence of the Aquitaine basin since Cretaceous times. *Bulletin de la Société géologique de France*, **6**(2), 295-306.

Dubreuilh, J., Capdeville, J.P., Farjanel, G., Karnay, G., Platel, J.P., Simon-Coinçon, R., 1995. Dynamique d'un comblement continental néogène et quaternaire: l'exemple du bassin d'Aquitaine. *Géol. France* 3–26.

Ducoux, M., Jolivet, L., Callot, J. P., Aubourg, C., Masini, E., Lahfid, A., ... & Baudin, T., 2019. The Nappe des Marbres unit of the Basque-Cantabrian Basin: the tectono-thermal evolution of a fossil hyperextended rift basin. *Tectonics*, **38**(11), 3881-3915.

Ducoux, M., Jolivet, L., Cagnard, F., & Baudin, T., 2021. Basement-cover decoupling during the inversion of a hyperextended basin: Insights from the Eastern Pyrenees. *Tectonics*, e2020TC006512.

Dupéron-Laudoueneix, M., Pons, D., 1985. Nouvelle étude de Mesembrioxylon libanoticum Edwards (Conifère du Mésozoïque supérieur) ; intérêts paléogéographique, biostratigraphique et paléoclimatique. *Plant Biosyst.* **119**, 151–166.

Einsele, G., 2000. *Sedimentary basins: evolution, facies, and sediment budget*. Springer Science & Business Media.

England, P., 1981. Metamorphic pressure estimates and sediment volumes for the Alpine orogeny: an independent control on geobarometers? *Earth Planet. Sci. Lett.* **56**, 387–397.

Fabriès, J., Lorand, J. P., Bodinier, J. L., & Dupuy, C., 1991. Evolution of the upper mantle beneath the Pyrenees: evidence from orogenic spinel lherzolite massifs. *Journal of Petrology*, 2, 55-76.

Fabriès, J., Lorand, J. P., & Bodinier, J. L., 1998. Petrogenetic evolution of orogenic lherzolite massifs in the central and western Pyrenees. *Tectonophysics*, **292**(1-2), 145-167.

Fillon, C., van der Beek, P., 2012. Post-orogenic evolution of the southern Pyrenees: Constraints from inverse thermo-kinematic modelling of low-temperature thermochronology data. *Basin Res.* **24**, 418–436.

Fillon, C., Pedreira, D., Van Der Beek, P.A., Huismans, R.S., Barbero, L., Pulgar, J.A., 2016. Alpine exhumation of the central Cantabrian mountains, northwest Spain. *Tectonics* **35**, 339–356.

Fillon, C., Mouthereau, F., Calassou, S., Pik, R., Bellahsen, N., Gautheron, C., ... & van der Beek, P., 2021. Post-orogenic exhumation in the western Pyrenees: evidence for extension driven by pre-orogenic inheritance. *Journal of the Geological Society*, **178**(2).

Fitzgerald, P.G., Muñoz, J.A., Coney, P.J., Baldwin, S.L., 1999. Asymmetric exhumation across the Pyrenean orogen: implications for the tectonic evolution of a collisional orogen. *Earth Planet. Sci. Lett.* **173**, 157–170.

Ford, M., Hemmer, L., Vacherat, A., Gallagher, K., & Christophoul, F., 2016. Retro-wedge foreland basin evolution along the ECORS line, eastern Pyrenees, France. *Journal of the Geological Society*, **173**(3), 419-437.

Foreman, B. Z., Heller, P. L., & Clementz, M. T., 2012. Fluvial response to abrupt global warming at the Palaeocene/Eocene boundary. *Nature*, **491**(7422), 92-95.

Gallagher, K., Charvin, K., Nielsen, S., Sambridge, M., & Stephenson, J., 2009. Markov chain Monte Carlo (MCMC) sampling methods to determine optimal models, model resolution and model choice for Earth Science problems. *Marine and Petroleum Geology*, **26**(4), 525-535.

Gallastegui, J., Pulgar, J.A., Gallart, J., 2002. Initiation of an active margin at the North Iberian continent-ocean transition. *Tectonics* **21**, 11–15.

Galloway, W.E., Whiteaker, T.L., Ganey-Curry, P., 2011. History of Cenozoic North American drainage basin evolution, sediment yield, and accumulation in the Gulf of Mexico basin. *Geosphere* **7**, 938–973.

Galloway, W.E., Williams, T.A., 1991. Sediment accumulation rates in time and space: Paleogene genetic stratigraphic sequences of the northwestern Gulf of Mexico basin. *Geology* **19**, 986–989.

Garcia-Castellanos, D., Vergés, J., Gaspar-Escribano, J., & Cloetingh, S., 2003. Interplay between tectonics, climate, and fluvial transport during the Cenozoic evolution of the Ebro Basin (NE Iberia). *Journal of Geophysical Research: Solid Earth*, **108**(B7).

Garcia-Castellanos, D., & Larrasoaña, J. C., 2015. Quantifying the post-tectonic topographic evolution of closed basins: The Ebro basin (northeast Iberia). *Geology*, **43(8**), 663-666.

Garzanti, E., 2019. The Himalayan Foreland Basin from collision onset to the present: A sedimentary–petrology perspective. *Geological Society, London, Special Publications*, **483(1)**, 65-122.

Gibson, M., Sinclair, H. D., Lynn, G. J., & Stuart, F. M., 2007. Late-to post-orogenic exhumation of the Central Pyrenees revealed through combined thermochronological data and modelling. *Basin Research*, **19(3)**, 323-334.

Gómez, M., Vergés, J., Riaza, C., 2002. Inversion tectonics of the northern margin of the Basque Cantabrian Basin. *Bull. la Société géologique Fr.* **173**, 449–459.

Goodbred Jr, S. L., & Kuehl, S. A., 2000. The significance of large sediment supply, active tectonism, and eustasy on margin sequence development: Late Quaternary stratigraphy and evolution of the Ganges–Brahmaputra delta. *Sedimentary Geology*, **133(3-4)**, 227-248.

Guillocheau, F., Brault, N., Thomas, E., Barbarand, J., Bonnet, S., Bourquin, S., Estéoule-Choux, J., Guennoc, P., Menier, D., Neraudeau, D., Proust, J.-N., Wyns, R., 2003. Histoire géologique du Massif armoricain depuis 140 Ma (Crétacé-Actuel). *Bulletin d'Information des Géologues du Bassin de Paris*, **40(1)**, 13-28.

Guillocheau, F., Rouby, D., Robin, C., Helm, C., Rolland, N., Carlier, L. E., Braun, J. (2012). Quantification and causes of the terrigeneous sediment budget at the scale of a continental margin: A new method applied to the Namibia-South Africa margin. *Basin Research*, ***24***, 3–30.

Gunnell, Y., Calvet, M., Brichau, S., Carter, A., Aguilar, J. P., & Zeyen, H., 2009. Low long-term erosion rates in high-energy mountain belts: Insights from thermo-and biochronology in the Eastern Pyrenees. *Earth and Planetary Science Letters,* **278(3-4)**, 208-218.

Hay, W.W., Shaw, C.A., Wold, C.N., 1989. Mass-balanced paleogeographic reconstructions. *Geol. Rundschau* **78**, 207–242.

Hay, W.W., Wold, C.N., 1990. Relation of selected mineral deposits to the mass/age distribution of Phanerozoic sediments. *Geol. Rundschau* **79**, 495–512.

Herman, F., Seward, D., Valla, P. G., Carter, A., Kohn, B., Willett, S. D., & Ehlers, T. A., 2013. Worldwide acceleration of mountain erosion under a cooling climate. *Nature*, **504**(7480), 423-426.

Herman, F., Champagnac, J.-D., 2016. Plio-Pleistocene increase of erosion rates in mountain belts in response to climate change. *Terra Nov.* **28**, 2–10.

Hinderer, M., 2012. From gullies to mountain belts: a review of sediment budgets at various scales. *Sedimentary Geology*, **280**, 21-59.

Iglesias, J., 2009. Sedimentation on the cantabrian continental margin from late oligocene to quaternary.

Jammes, S., Manatschal, G., Lavier, L., & Masini, E., 2009. Tectonosedimentary evolution related to extreme crustal thinning ahead of a propagating ocean: Example of the western Pyrenees. *Tectonics*, **28**(4).

Jolivet, M., Labaume, P., Monié, P., Brunel, M., Arnaud, N., & Campani, M., 2007. Thermochronology constraints for the propagation sequence of the south Pyrenean basement thrust system (France-Spain). *Tectonics*, **26**(5).

Ketcham, R. A., 2005. Forward and inverse modeling of low-temperature thermochronometry data. *Reviews in mineralogy and geochemistry*, **58**(1), 275-314.

Kuhlemann, J., Frisch, W., Székely, B., Dunkl, I., Kázmér, M., 2002. Post-collisional sediment budget history of the Alps: tectonic versus climatic control. *Int. J. Earth Sci.* **91**, 818–837.

Kuhlemann, J., 2000. Post-collisional sediment budget of circum-Alpine basins (Central Europe). *Mem. Sci. Geol. Padova* **52**, 1–91.

Labaume, P., Meresse, F., Jolivet, M., & Teixell, A., 2016. Exhumation sequence of the basement thrust units in the west-central Pyrenees. Constraints from apatite fission track analysis. *Geogaceta*, **60**, 11-14.

Lagabrielle, Y., & Bodinier, J. L., 2008. Submarine reworking of exhumed subcontinental mantle rocks: field evidence from the Lherz peridotites, French Pyrenees. *Terra Nova*, **20**(1), 11-21.

Lagabrielle, Y., Labaume, P., de Saint Blanquat, M., 2010. Mantle exhumation, crustal denudation, and gravity tectonics during Cretaceous rifting in the Pyrenean realm (SW Europe): Insights from the geological setting of the lherzolite bodies. *Tectonics* **29**.

Leroux, E., Rabineau, M., Aslanian, D., Gorini, C., Molliex, S., Bache, F., & Suc, J. P., 2017. High-resolution evolution of terrigenous sediment yields in the Provence Basin during the last 6 Ma: relation with climate and tectonics. *Basin Research*, **29**(3), 305-339.

Macchiavelli, C., Vergés, J., Schettino, A., Fernàndez, M., Turco, E., Casciello, E., Torne, M., Pierantoni, P.P., Tunini, L., 2017. A new southern North Atlantic isochron map: Insights into the drift of the Iberian plate since the Late Cretaceous. *J. Geophys. Res. Solid Earth* **122**, 9603–9626.

Masini, E., Manatschal, G., Tugend, J., Mohn, G., Flament, J.-M., 2014. The tectono-sedimentary evolution of a hyper-extended rift basin: the example of the Arzacq--Mauléon rift system (Western Pyrenees, SW France). *Int. J. Earth Sci.* **103**, 1569–1596.

Maurel, O., Monie, P., Pik, R., Arnaud, N., Brunel, M., & Jolivet, M., 2008. The Meso-Cenozoic thermo-tectonic evolution of the Eastern Pyrenees: an 40 Ar/39 Ar fission track and (U–Th)/He thermochronological study of the Canigou and Mont-Louis massifs. *International Journal of Earth Sciences*, **97(3)**, 565-584.

Metcalf, J. R., Fitzgerald, P. G., Baldwin, S. L., & Muñoz, J. A., 2009. Thermochronology of a convergent orogen: Constraints on the timing of thrust faulting and subsequent exhumation of the Maladeta Pluton in the Central Pyrenean Axial Zone. *Earth and Planetary Science Letters*, **287(3-4)**, 488-503.

Métivier, F., Gaudemer, Y., Tapponnier, P., Klein, M., 1999. Mass accumulation rates in Asia during the Cenozoic. *Geophys. J. Int.* **137**, 280–318.

Michael, N.A., Whittaker, A.C., Allen, P.A., 2013. The functioning of sediment routing systems using a mass balance approach: Example from the Eocene of the southern Pyrenees. *J. Geol.* **121**, 581–606.

Michael, N.A., Carter, A., Whittaker, A.C., Allen, P.A., 2014. Erosion rates in the source region of an ancient sediment routing system: Comparison of depositional volumes with thermochronometric estimates. *J. Geol. Soc. London.* **171**, 401–412.

Michael, N.A., Whittaker, A.C., Carter, A., Allen, P.A., 2014. Volumetric budget and grain-size fractionation of a geological sediment routing system: Eocene Escanilla Formation, south-central Pyrenees. *Bull. Geol. Soc. Am.* **126**, 585–599.

Molnar, P., 2004. Late Cenozoic increase in accumulation rates of terrestrial sediment: How might climate change have affected erosion rates? *Annu. Rev. Earth Planet. Sci.* **32**, 67–89.

Molnar, P., England, P., 1990. Late Cenozoic uplift of mountain ranges and global climate change: chicken or egg? *Nature* **346**, 29–34.

Molnar, P., Lyon-Caen, H., 1988. Some simple physical aspects of the support, structure, and evolution of mountain belts. *Process. Cont. lithospheric Deform.* **218**, 179–207.

Mouchené, M., van der Beek, P., Mouthereau, F., & Carcaillet, J., 2017. Controls on Quaternary incision of the Northern Pyrenean foreland: Chronological and geomorphological constraints from the Lannemezan megafan, SW France. *Geomorphology*, **281**, 78-93.

Mouthereau, F., Filleaudeau, P. Y., Vacherat, A., Pik, R., Lacombe, O., Fellin, M. G., ... & Masini, E., 2014. Placing limits to shortening evolution in the Pyrenees: Role of margin architecture and implications for the Iberia/Europe convergence. *Tectonics*, **33(12)**, 2283-2314.

Muñoz, J. A., 1992. Evolution of a continental collision belt: ECORS-Pyrenees crustal balanced cross-section. In *Thrust tectonics* (pp. 235-246). Springer, Dordrecht.

Najman, Y., & Garzanti, E., 2000. Reconstructing early Himalayan tectonic evolution and paleogeography from Tertiary foreland basin sedimentary rocks, northern India. *Geological Society of America Bulletin*, **112(3)**, 435-449.

Nelson, C. H., 1990. Estimated post-Messinian sediment supply and sedimentation rates on the Ebro continental margin, Spain. *Marine Geology*, *95*(3-4), 395-418.

Ortiz, A., Guillocheau, F., Lasseur, E., Briais, J., Robin, C., Serrano, O., Fillon, C., 2020. Sediment routing system and sink preservation during the post-orogenic evolution of a retro-foreland basin: The case example of the North Pyrenean (Aquitaine, Bay of Biscay) Basins. *Mar. Pet. Geol.* **112**, 104085.

Pedreira, D., Afonso, J.C., Pulgar, J.A., Gallastegui, J., Carballo, A., Fernàndez, M., Garcia-Castellanos, D., Jiménez-Munt, I., Semprich, J., Garcia-Moreno, O., 2015. Geophysical-petrological modeling of the lithosphere beneath the Cantabrian Mountains and the North-Iberian margin: Geodynamic implications. *Lithos* **230**, 46–68.

Roest, W.R., Srivastava, S.P., 1991. Kinematics of the plate boundaries between Eurasia, Iberia, and Africa in the North Atlantic from the Late Cretaceous to the present. *Geology* **19**, 613–616.

Roure, F., Choukroune, P., Berastegui, X., Munoz, J. A., Villien, A., Matheron, P., . & Deramond, J., 1989. ECORS deep seismic data and balanced cross sections: Geometric constraints on the evolution of the Pyrenees. *Tectonics*, **8(**1), 41-50.

Saspiturry, N., Razin, P., Baudin, T., Serrano, O., Issautier, B., Lasseur, E., Allanic, C., Thinon, I., Leleu, S., 2019. Symmetry vs. asymmetry of a hyper-thinned rift: example of the Mauléon Basin (Western Pyrenees, France). *Mar. Pet. Geol.* **104**, 86–105.

Schettino, A., Turco, E., 2011. Tectonic history of the western Tethys since the Late Triassic. *Bulletin*, **123**(1-2), 89–105.

Schlunegger, F., Melzer, J., & Tucker, G., 2001. Climate, exposed source-rock lithologies, crustal uplift and surface erosion: a theoretical analysis calibrated with data from the

Alps/North Alpine Foreland Basin system. *International Journal of Earth Sciences,* **90(3)**, 484-499.

Schlunegger, F., & Mosar, J., 2011. The last erosional stage of the Molasse Basin and the Alps. *International Journal of Earth Sciences*, **100**(5), 1147-1162.

Schlunegger, F., & Norton, K. P., 2015. Climate vs. tectonics: the competing roles of Late Oligocene warming and Alpine orogenesis in constructing alluvial megafan sequences in the North Alpine foreland basin. *Basin research,* **27**(2), 230-245.

Schmid, S. M., Pfiffner, O. A., Froitzheim, N., Schönborn, G., & Kissling, E., 1996. Geophysical-geological transect and tectonic evolution of the Swiss-Italian Alps. *Tectonics*, **15**(5), 1036-1064.

Serrano, O., 2001. Le Crétacé Supérieur-Paléogène du Bassin Compressif Nord-Pyrénéen (Bassin de l'Adour). Sédimentologie, Stratigraphie, Géodynamique. Université Rennes 1.

Serrano, O., Guillocheau, F., & Leroy, E., 2001. Évolution du bassin compressif Nord-Pyrénéen au Paléogène (bassin de l'Adour): contraintes stratigraphiques. *Comptes Rendus de l'Académie des Sciences-Series IIA-Earth and Planetary Science*, **332**(1), 37-44.

Sinclair, H.D., Gibson, M., Naylor, M., Morris, R.G., 2005. Asymmetric growth of the Pyrenees revealed through measurement and modeling of orogenic fluxes. *Am. J. Sci.* **305**, 369–406.

Sztrákos, K., Gély, J. P., Blondeau, A., & Muller, C., 1998. L'Eocène du Bassin sud-aquitain: lithostratigraphie, biostratigraphie et analyse séquentielle. *Géologie de la France*, (4), 57-105.

Sztrákos, K., & Steurbaut, E., 2017. Révision lithostratigraphique et biostratigraphique de l'Oligocène d'Aquitaine occidentale (France). *Geodiversitas*, **39**(4), 741-781.

Teixell, A., 1998. Crustal structure and orogenic material budget in the west central Pyrenees. *Tectonics*, **17(3)**, 395-406.

Ternois, S., Odlum, M., Ford, M., Pik, R., Stockli, D., Tibari, B., Vacherat, A., Bernard, V., 2019. Thermochronological evidence of early orogenesis, eastern Pyrenees, France. *Tectonics* **38**, 1308–1336.

Thinon, I., 1999. Structure profonde de la marge nord-Gascogne et du bassin armoricain. Brest.

Thinon, I., Fidalgo-González, L., Réhault, J.-P., Olivet, J.-L., 2001. Déformations pyrénéennes dans le golfe de Gascogne. *Comptes Rendus l'Académie des Sci. IIA-Earth Planet. Sci.* **332**, 561–568.

Tugend, J., Manatschal, G., Kusznir, N. J., Masini, E., Mohn, G., & Thinon, I., 2014. Formation and deformation of hyperextended rift systems: Insights from rift domain mapping in the Bay of Biscay-Pyrenees. *Tectonics*, **33**(7), 1239-1276.

Vacherat, A., Mouthereau, F., Pik, R., Bernet, M., Gautheron, C., Masini, E., ... & Lahfid, A., 2014. Thermal imprint of rift-related processes in orogens as recorded in the Pyrenees. *Earth and Planetary Science Letters*, **408**, 296-306.

Vacherat, A., Mouthereau, F., Pik, R., Bellahsen, N., Gautheron, C., Bernet, M., ... & Radal, J., 2016. Rift-to-collision transition recorded by tectonothermal evolution of the northern Pyrenees. *Tectonics*, **35(4)**, 907-933.

Van Rooij, D., Iglesias, J., Hernández-Molina, F.J., Ercilla, G., Gomez-Ballesteros, M., Casas, D., Llave, E., De Hauwere, A., Garcia-Gil, S., Acosta, J., others, 2010. The Le Danois Contourite Depositional System: interactions between the Mediterranean outflow water and the upper Cantabrian slope (North Iberian margin). *Mar. Geol.* **274**, 1–20.

Vergés, J., Fernàndez, M., & Martìnez, A., 2002. The Pyrenean orogen: pre-, syn-, and post-collisional evolution. *Journal of the Virtual Explorer*, **8**, 55-74.

Waldner, M., Bellahsen, N., Mouthereau, F., Bernet, M., Pik, R., Rosenberg, C. L., & Balvay, M., 2021. Central Pyrenees mountain building: constraints from new LT thermochronological data from the Axial Zone. *Tectonics*, e2020TC006614.

Watts, A. B., & Torné, M., 1992. Crustal structure and the mechanical properties of extended continental lithosphere in the Valencia trough (western Mediterranean). *Journal of the Geological Society*, **149(5)**, 813-827.

Watts, A.B., 2001. Isostasy and Flexure of the Lithosphere. *Cambridge University Press*.

Willett, S.D., 1999. Orogeny and orography: the effects of erosion on the structure of mountain belts. *J. Geophys. Res., Solid Earth* **104** (B12), 28957–28981.

Whipple, K.X., 2009. The influence of climate on the tectonic evolution of mountain belts. *Nat. Geosci.* **2**, 97–104.

Whitchurch, A. L., Carter, A., Sinclair, H. D., Duller, R. A., Whittaker, A. C., & Allen, P. A., 2011. Sediment routing system evolution within a diachronously uplifting orogen: Insights from detrital zircon thermochronological analyses from the South-Central Pyrenees. *American Journal of Science*, **311**(5), 442-482.

Wold, C.N., Hay, W.W., 1990. Estimating ancient sediment fluxes. *Am. J. Sci.* **290**, 1069–1089.

Zachos, J., Pagani, M., Sloan, L., Thomas, E., Billups, K., 2001. Trends, rhythms, and aberrations in global climate 65 Ma to present. *Science* **292**, 686–693.

Table 1 caption: Siliciclastic sediment volumes and rates values, with the uncertainties

Accumulated solid volumes, rates and associated variance for the Aquitaine Basin

Time interval	(Ma)	Volume (× 1 km³)	σ	Rate (× 1 km³ / Myr)	σ
Pliocene - Pleistocene	5.33 - 0	228.6	± 10.8	43.1	± 2.0
Aquitanian - Messinian	23.03 - 5.33	1 370.3	± 385.2	77.2	± 21.7
Rupelian - Chattian	33.9 - 23.03	7 894.7	± 1 949.9	726.2	± 179.3
Danian - Priabonian	66 - 33.9	16 545.6	± 5 563.1	515.4	± 173.3

Accumulated solid volumes, rates and associated variance for the southern Bay of Biscay

Time interval	(Ma)	Volume (× 1 km³)	σ	Rate (× 1 km³ / Myr)	σ
Pliocene - Pleistocene	5.33 - 0	16 445.0	± 5 929.1	3 084.2	± 1 111.9
Aquitanian - Messinian	23.03 - 5.33	7 301.3	± 2 231.5	411.8	± 125.9
Rupelian - Chattian	33.9 - 23.03	1 043.7	± 351.8	96.0	± 32.4
Danian - Priabonian	66 - 33.9	652.7	± 352.0	20.6	± 11.1

Accumulated solid volumes, rates and associated variance for the whole basins

Time interval	(Ma)	Volume (× 1 km³)	σ	Rate (× 1 km³ / Myr)	σ
Pliocene - Pleistocene	5.33 - 0	16 673.6	± 5 940.0	3 145.9	± 1 120.8
Aquitanian - Messinian	23.03 - 5.33	8 671.7	± 2 616.8	489.1	± 147.6
Rupelian - Chattian	33.9 - 23.03	8 938.4	± 2 301.7	822.3	± 211.7
Danian - Priabonian	66 - 33.9	17 198.3	± 5 915.2	535.8	± 184.3

Table 1

Table 2 caption: Percentage of carbonates for the studied time interval

Carbonate fraction for the Bay of Biscay

Time interval	(Ma)	Carbonate fraction (%)	σ
Pliocene - Pleistocene	5.33 - 0	7.5	± 7.5
Messinian	7.24 - 5.33	14	± 10
Aquitanian - Tortonian	23.03 - 7.24	18	± 10
Rupelian - Chattian	33.9 - 23.03	44	± 15
Danian - Priabonian	66 - 33.9	60	± 20

Carbonate fraction for the «Façade Atlantique» Basin

Time interval	(Ma)	Carbonate fraction (%)	σ
Pliocene - Pleistocene	5.33 - 0	5	± 5
Tortonian - Messinian	11.63 - 5.33	10	± 10
Langhian - Serravallian	15.97 - 11.63	20	± 20
Burdigalian	20.44 - 15.97	50	± 20
Aquitanian	23.03 - 20.44	60	± 30
Rupelian - Chattian	33.9 - 23.03	40	± 20
Priabonian	37.8 - 33.9	50	± 20
Danian - Bartonian	66 - 37.8	40	± 20

Carbonate fraction for the Arzacq Basin

Time interval	(Ma)	Carbonate fraction (%)	σ
Pliocene - Pleistocene	5.33 - 0	5	± 5
Tortonian - Messinian	11.63 - 5.33	10	± 10
Langhian - Serravallian	15.97 - 11.63	20	± 20
Burdigalian	20.44 - 15.97	50	± 20
Aquitanian	23.03 - 20.44	60	± 30
Rupelian - Chattian	33.9 - 23.03	20	± 10
Priabonian	37.8 - 33.9	20	± 10
Danian - Bartonian	66 - 37.8	40	± 20

Carbonate fraction for the Carcassonne Basin

Time interval	(Ma)	Carbonate fraction (%)	σ
Pliocene - Pleistocene	5.33 - 0	5	± 5
Tortonian - Messinian	11.63 - 5.33	10	± 10
Langhian - Serravallian	15.97 - 11.63	20	± 20
Burdigalian	20.44 - 15.97	50	± 20
Aquitanian	23.03 - 20.44	60	± 30
Rupelian - Chattian	33.9 - 23.03	25	± 20
Priabonian	37.8 - 33.9	20	± 20
Danian - Bartonian	66 - 37.8	40	± 20

Carbonate fraction for the Tarbes Basin

Time interval	(Ma)	Carbonate fraction (%)	σ
Pliocene - Pleistocene	5.33 - 0	5	± 5
Tortonian - Messinian	11.63 - 5.33	10	± 10
Langhian - Serravallian	15.97 - 11.63	20	± 20
Burdigalian	20.44 - 15.97	50	± 20
Aquitanian	23.03 - 20.44	60	± 30
Rupelian - Chattian	33.9 - 23.03	20	± 10
Priabonian	37.8 - 33.9	15	± 10
Danian - Bartonian	66 - 37.8	40	± 20

Carbonate fraction for the Aquitaine platform

Time interval	(Ma)	Carbonate fraction (%)	σ
Pliocene - Pleistocene	5.33 - 0	5	± 5
Tortonian - Messinian	11.63 - 5.33	10	± 10
Langhian - Serravallian	15.97 - 11.63	20	± 20
Burdigalian	20.44 - 15.97	50	± 20
Aquitanian	23.03 - 20.44	60	± 30
Rupelian - Chattian	33.9 - 23.03	20	± 10
Priabonian	37.8 - 33.9	15	± 10
Danian - Bartonian	66 - 37.8	40	± 20

Carbonate fraction for the Castres Basin

Time interval	(Ma)	Carbonate fraction (%)	σ
Pliocene - Pleistocene	5.33 - 0	5	± 5
Tortonian - Messinian	11.63 - 5.33	10	± 10
Langhian - Serravallian	15.97 - 11.63	20	± 20
Burdigalian	20.44 - 15.97	50	± 20
Aquitanian	23.03 - 20.44	60	± 30
Rupelian - Chattian	33.9 - 23.03	40	± 20
Priabonian	37.8 - 33.9	40	± 20
Danian - Bartonian	66 - 37.8	40	± 20

Carbonate fraction for the Tartas Mirande Basin

Time interval	(Ma)	Carbonate fraction (%)	σ
Pliocene - Pleistocene	5.33 - 0	5	± 5
Tortonian - Messinian	11.63 - 5.33	10	± 10
Langhian - Serravallian	15.97 - 11.63	20	± 20
Burdigalian	20.44 - 15.97	50	± 20
Aquitanian	23.03 - 20.44	60	± 30
Rupelian - Chattian	33.9 - 23.03	30	± 20
Priabonian	37.8 - 33.9	50	± 10
Danian - Bartonian	66 - 37.8	40	± 20

Table 2

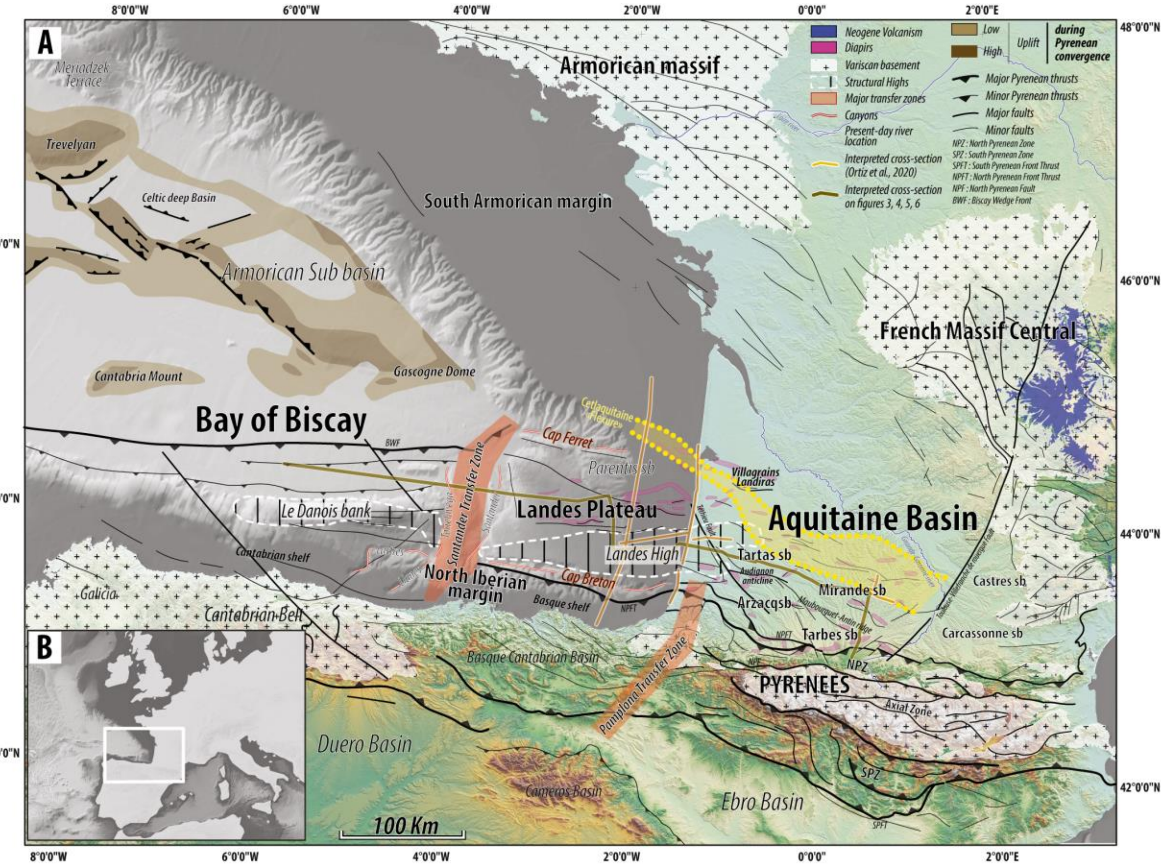
A
B
8°0'0"W
6°0'0"W
4°0'0"W
2°0'0"W
0°0'0"
2°0'0"E
48°0'0"N
46°0'0"N
44°0'0"N
42°0'0"N
Neogene Volcanism
Diapirs
Variscan basement
Structural Highs
Major transfer zones
Canyons
Present-day river location
Interpreted cross-section (Ortiz et al., 2020)
Interpreted cross-section on figures 3, 4, 5, 6
Low
High
Uplift
during Pyrenean convergence
Major Pyrenean thrusts
Minor Pyrenean thrusts
Major faults
Minor faults
NPZ : North Pyrenean Zone
SPZ : South Pyrenean Zone
SPFT : South Pyrenean Front Thrust
NPFT : North Pyrenean Front Thrust
NPF : North Pyrenean Fault
BWF : Biscay Wedge Front
Armorican massif
Trevelyan
Celtic deep Basin
South Armorican margin
Armorican Sub basin
Cantabria Mount
Gascogne Dome
French Massif Central
Bay of Biscay
BWF
Cap Ferret
Parentis sb
Villagrains Landiras
Le Danois bank
Santander Transfer Zone
Landes Plateau
Aquitaine Basin
Landes High
Tartas sb
Cantabrian shelf
North Iberian margin
Cap Breton
Arzacqsb
Mirande sb
Castres sb
Galicia
Cantabrian Belt
Basque shelf
NPFT
Tarbes sb
Carcassonne sb
Basque Cantabrian Basin
Pamplona Transfer Zone
NPZ
PYRENEES
Axial Zone
Duero Basin
Cameros Basin
Ebro Basin
SPZ
SPFT
100 Km

Figure 1

Figure 1: A: Main physiographic and structural features and available dataset of seismic reflection lines in the Aquitaine Basin, Landes Plateau and Biscay Bay deep-basin. B: Location of the studied area in Europe.

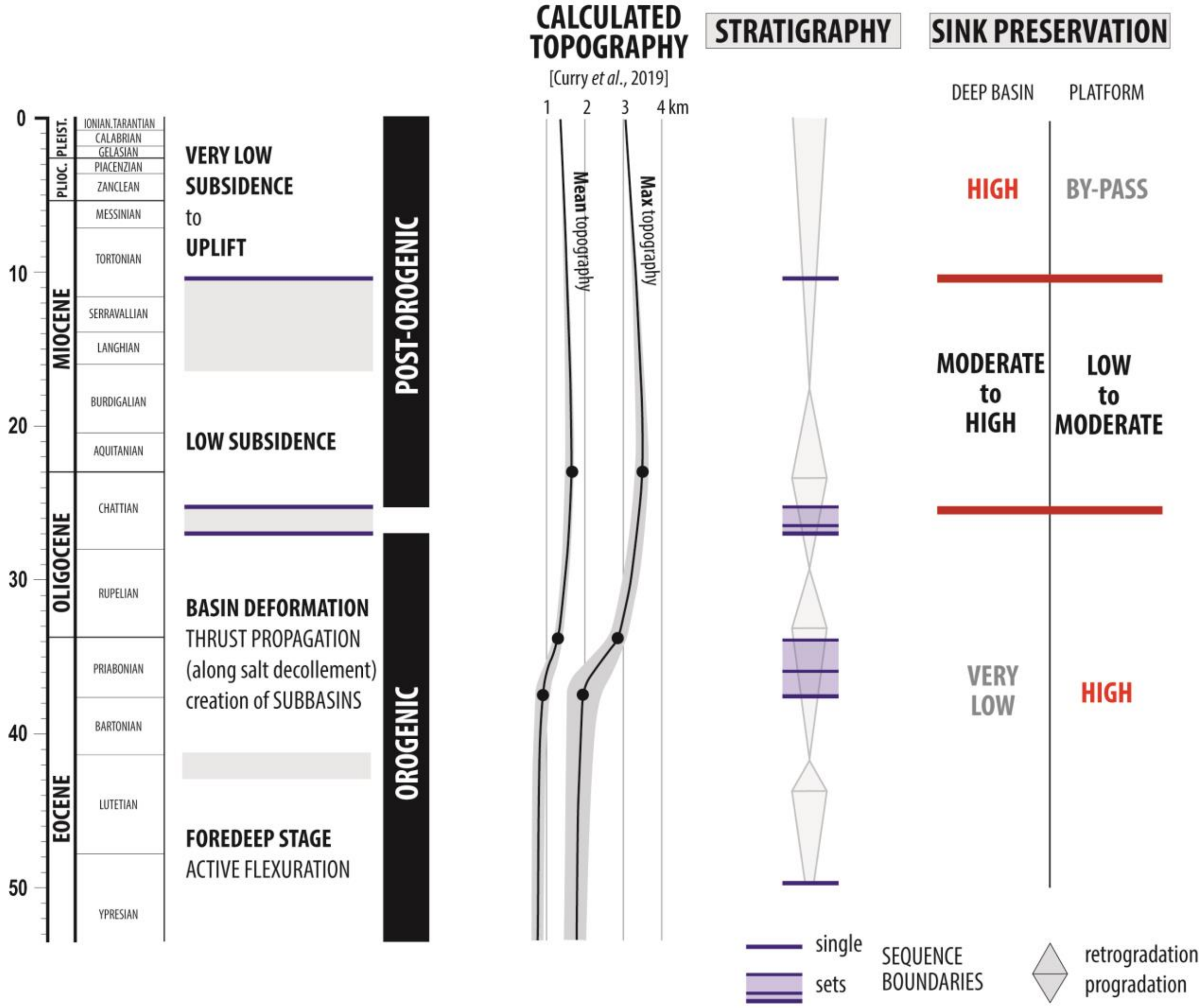

912 **Figure 2**

913

Figure 2: Synthetic chart of the main events (deformation, topography, sediment routing) of the Aquitaine Basin to deep Biscay Bay Basin sedimentary system

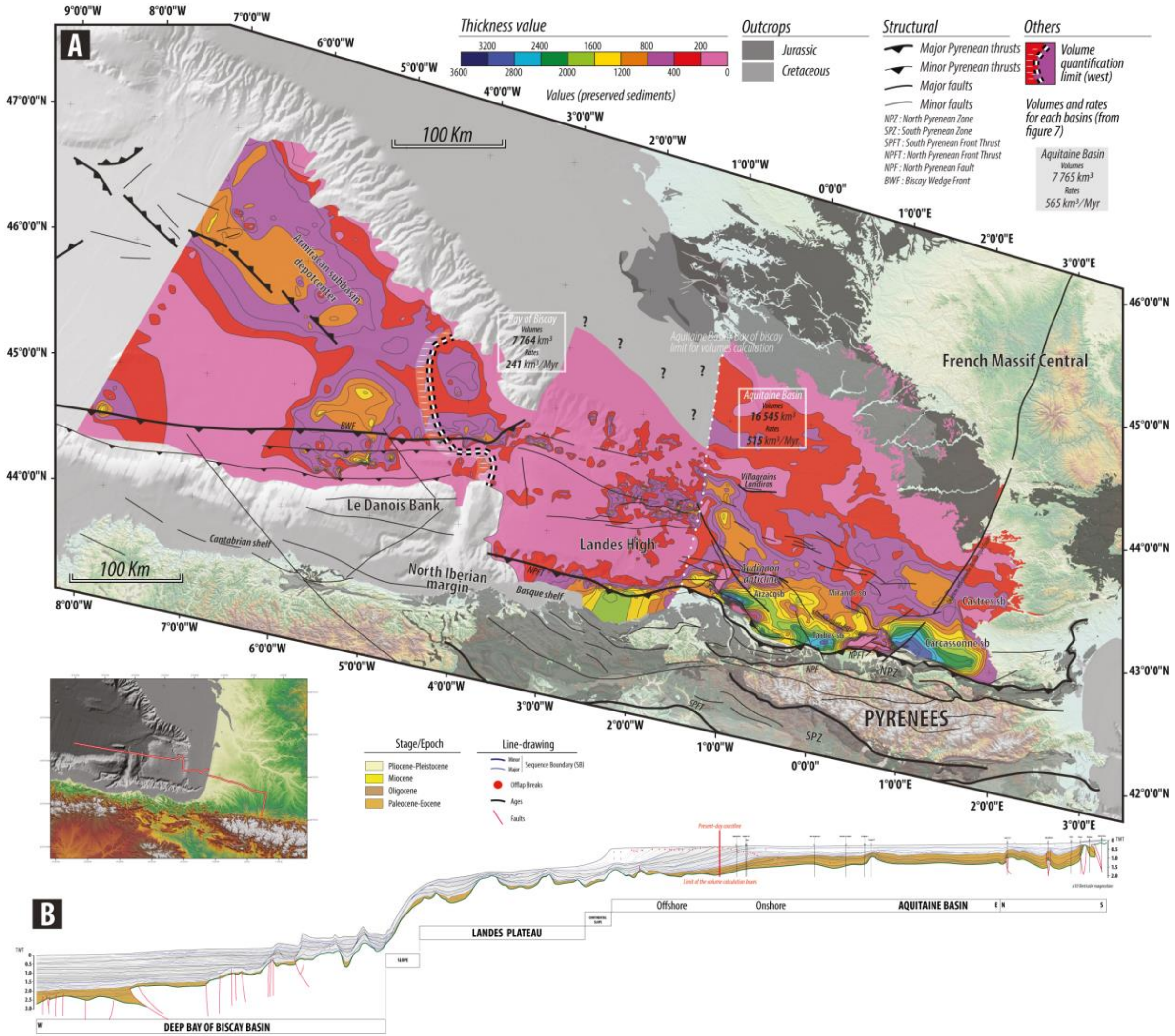
A
Thickness value
Values (preserved sediments)
Outcrops
Jurassic
Cretaceous
Structural
Major Pyrenean thrusts
Minor Pyrenean thrusts
Major faults
Minor faults
NPZ : North Pyrenean Zone
SPZ : South Pyrenean Zone
SPFT : South Pyrenean Front Thrust
NPFT : North Pyrenean Front Thrust
NPF : North Pyrenean Fault
BWF : Biscay Wedge Front
Others
Volume quantification limit (west)
Volumes and rates for each basins (from figure 7)
Aquitaine Basin
Volumes
7 765 km³
Rates
565 km³/Myr
Bay of Biscay
7 764 km³
241 km³/Myr
Aquitaine Basin
16 545 km³
515 km³/Myr
French Massif Central
Le Danois Bank
Landes High
North Iberian margin
Basque shelf
Cantabrian shelf
PYRENEES
100 Km
B
Stage/Epoch
Pliocene-Pleistocene
Miocene
Oligocene
Paleocene-Eocene
Line-drawing
Sequence Boundary (SB)
Offlap Breaks
Ages
Faults
Offshore
Onshore
AQUITAINE BASIN
LANDES PLATEAU
DEEP BAY OF BISCAY BASIN

937 **Figure 3**

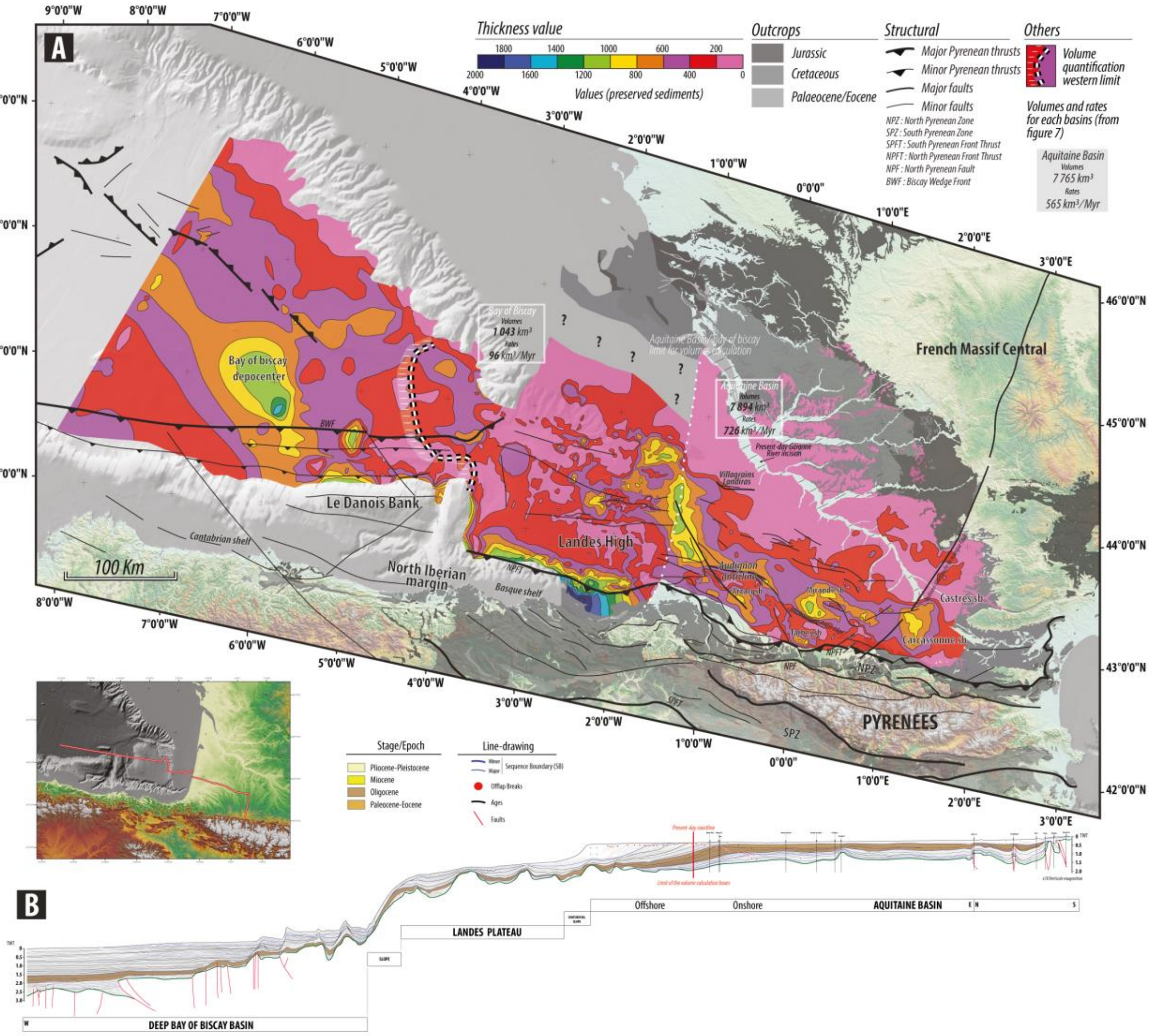

A
Thickness value
Values (preserved sediments)
Outcrops
Jurassic
Cretaceous
Palaeocene/Eocene
Structural
Major Pyrenean thrusts
Minor Pyrenean thrusts
Major faults
Minor faults
NPZ : North Pyrenean Zone
SPZ : South Pyrenean Zone
SPFT : South Pyrenean Front Thrust
NPFT : North Pyrenean Front Thrust
NPF : North Pyrenean Fault
BWF : Biscay Wedge Front
Others
Volume quantification western limit
Volumes and rates for each basins (from figure 7)
Aquitaine Basin
Volumes 7 765 km³
Rates 565 km³/Myr
Bay of Biscay
Volumes 1 043 km³
Rates 96 km³/Myr
Aquitaine Basin
Volumes 7 894 km³
Rates 726 km³/Myr
Bay of biscay depocenter
French Massif Central
Le Danois Bank
Landes High
North Iberian margin
Cantabrian shelf
Basque shelf
PYRENEES
100 Km
B
Stage/Epoch
Pliocene-Pleistocene
Miocene
Oligocene
Paleocene-Eocene
Line-drawing
Sequence Boundary (SB)
Offlap Breaks
Ages
Faults
DEEP BAY OF BISCAY BASIN
LANDES PLATEAU
Offshore
Onshore
AQUITAINE BASIN

938 **Figure 4**

Figure 3: A: Palaeocene-Eocene preserved sediment thickness (isopach, meters) map. The volume quantification western limit is according to the deep sea fan location (Cremer, 1983; Iglesias, 2009). B: interpreted cross-section from the proximal Aquitaine Basin part to the deep Bay of Biscay Basin, the considered period (isopach map) is highlighted by colour in the cross-section.

Figure 4: A: Oligocene preserved sediment thickness (isopach, meters) map. The volume quantification western limit is according to the deep sea fan location (Cremer, 1983; Iglesias, 2009). B: interpreted cross-section from the proximal Aquitaine Basin part to the deep Bay of Biscay Basin, the considered period (isopach map) is highlighted by colour in the cross-section.

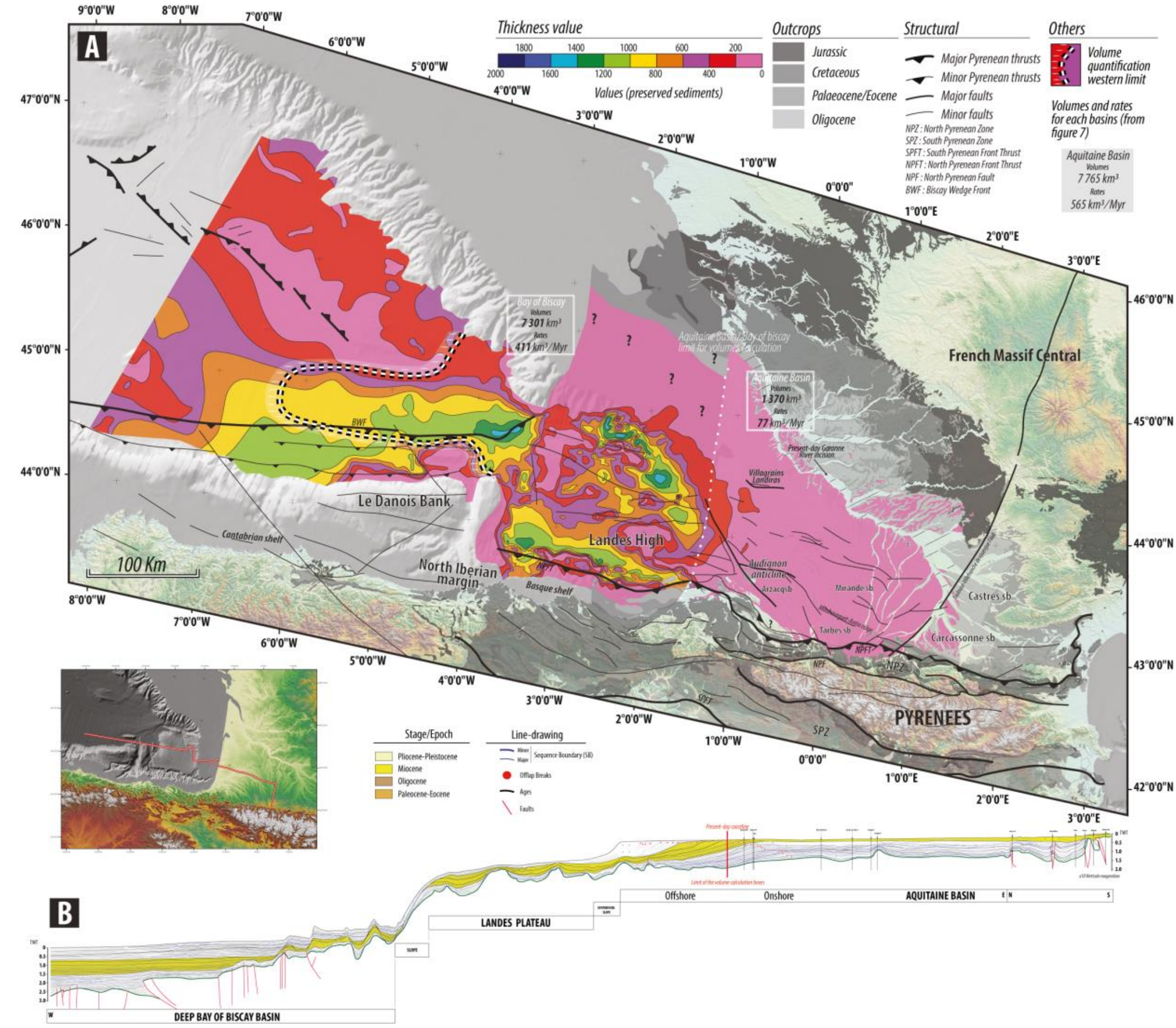

A
Thickness value
Values (preserved sediments)
Outcrops
Jurassic
Cretaceous
Palaeocene/Eocene
Oligocene
Structural
Major Pyrenean thrusts
Minor Pyrenean thrusts
Major faults
Minor faults
NPZ : North Pyrenean Zone
SPZ : South Pyrenean Zone
SPFT : South Pyrenean Front Thrust
NPFT : North Pyrenean Front Thrust
NPF : North Pyrenean Fault
BWF : Biscay Wedge Front
Others
Volume quantification western limit
Volumes and rates for each basins (from figure 7)
Aquitaine Basin
7 765 km³
565 km³/Myr
Bay of Biscay
7 301 km³
411 km³/Myr
Aquitaine Basin
1 370 km³
77 km³/Myr
French Massif Central
Le Danois Bank
Landes High
North Iberian margin
Cantabrian shelf
Basque shelf
PYRENEES
100 Km
Castres sb
Carcassonne sb
Stage/Epoch
Pliocene-Pleistocene
Miocene
Oligocene
Paleocene-Eocene
Line-drawing
B
DEEP BAY OF BISCAY BASIN
LANDES PLATEAU
Offshore
Onshore
AQUITAINE BASIN

Figure 5

Figure 5: A: Miocene preserved sediment thickness (isopach, meters) map. The volume quantification western limit is according to the deep sea fan location (Cremer, 1983; Iglesias, 2009). B: interpreted cross-section from the proximal Aquitaine Basin part to the deep Bay of Biscay Basin, the considered period (isopach map) is highlighted by colour in the cross-section.

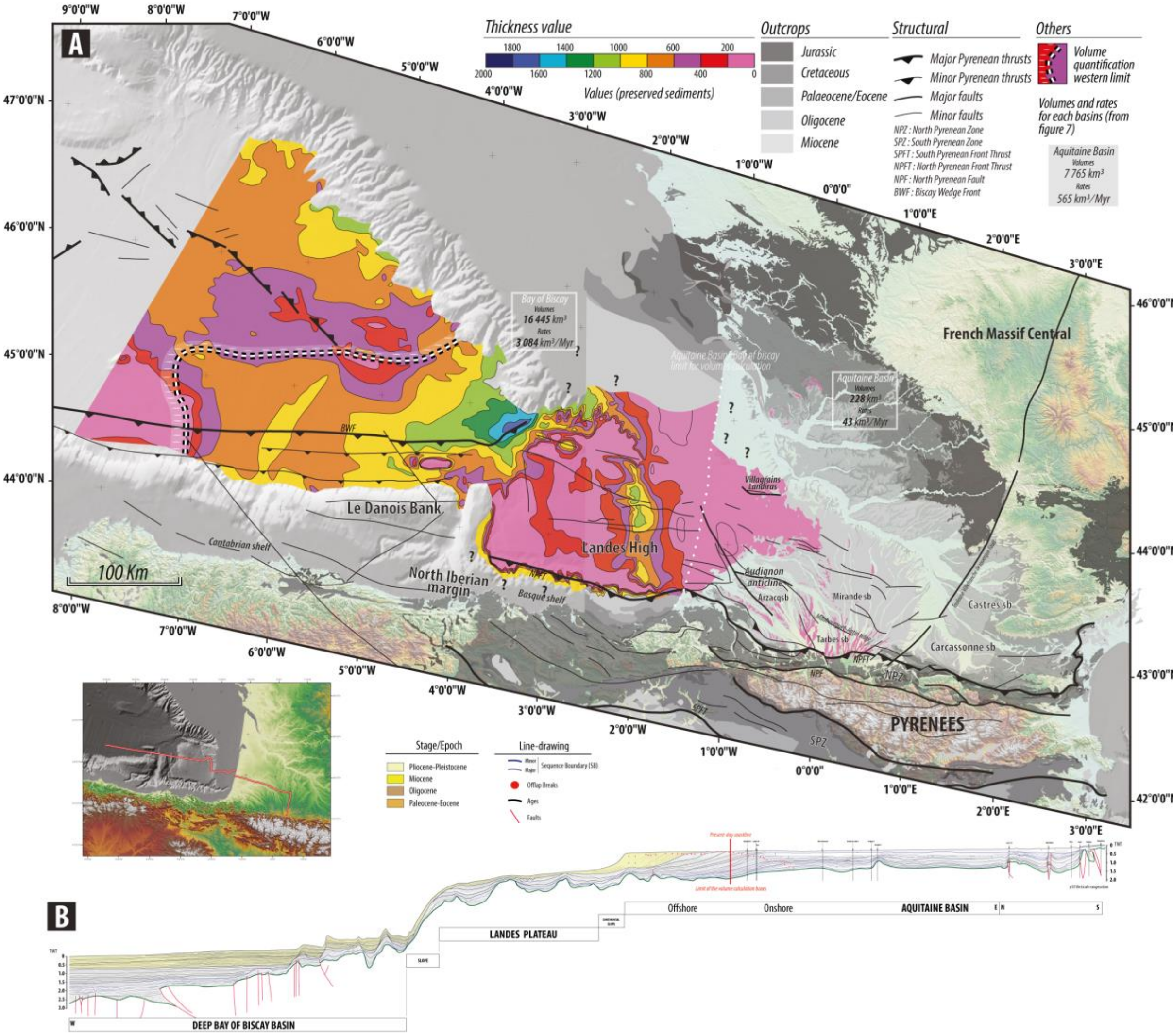

1019 **Figure 6**

1020

Figure 6: A: Pliocene-Pleistocene preserved sediment thickness (isopach, meters) map. The volume quantification western limit is according to the deep sea fan location (Cremer, 1983; Iglesias, 2009, Brocheray et al., 2014). B: interpreted cross-section from the proximal Aquitaine Basin part to the deep Bay of Biscay Basin, the considered period (isopach map) is highlighted by colour in the cross-section.

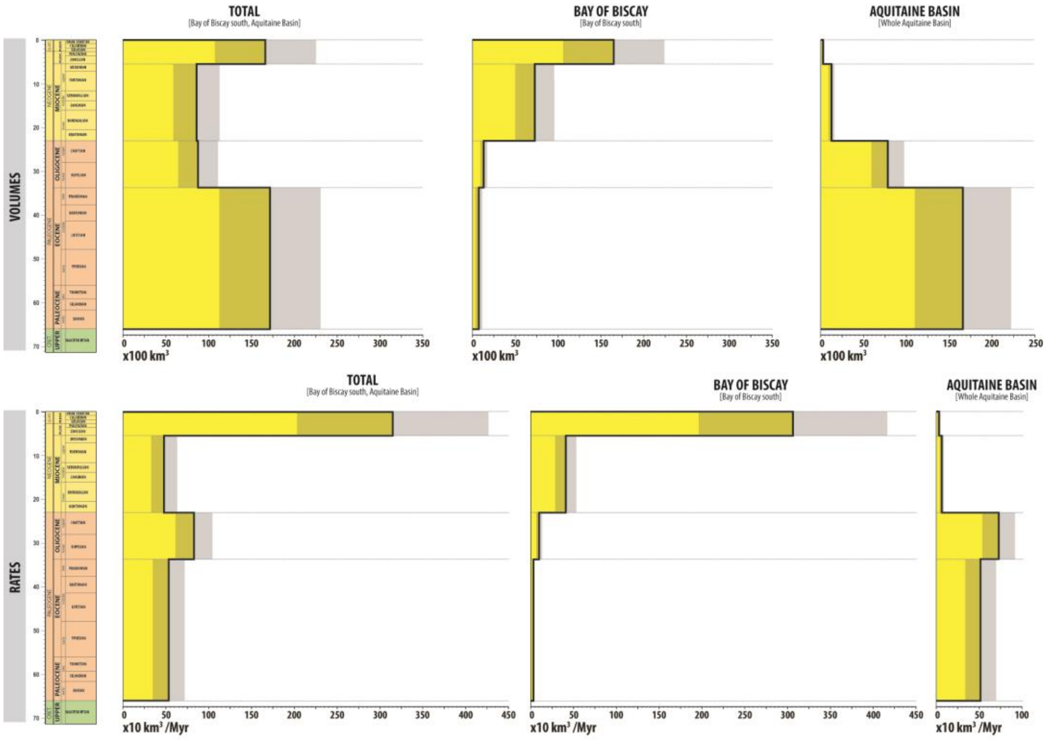

VOLUMES
RATES
TOTAL
[Bay of Biscay south, Aquitaine Basin]
BAY OF BISCAY
[Bay of Biscay south]
AQUITAINE BASIN
[Whole Aquitaine Basin]
MIOCENE
OLIGOCENE
EOCENE
PALEOCENE
UPPER
x100 km³
x10 km³ /Myr

Figure 7

Figure 7: Siliciclastic sedimentation volumes and rates of the Aquitaine Basin and Bay of Biscay.

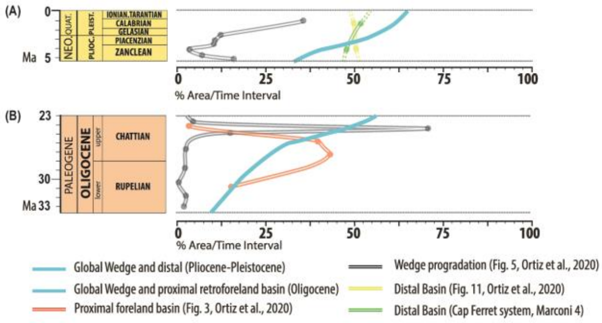
(A)
0
5
Ma
NEO
QUAT.
PLIOC.
PLEIST.
IONIAN,TARANTIAN
CALABRIAN
GELASIAN
PIACENZIAN
ZANCLEAN
0
25
50
75
100
% Area/Time Interval
(B)
23
30
Ma 33
PALEOGENE
OLIGOCENE
upper
lower
CHATTIAN
RUPELIAN
0
25
50
75
100
% Area/Time Interval
Global Wedge and distal (Pliocene-Pleistocene)
Global Wedge and proximal retroforeland basin (Oligocene)
Proximal foreland basin (Fig. 3, Ortiz et al., 2020)
Wedge progradation (Fig. 5, Ortiz et al., 2020)
Distal Basin (Fig. 11, Ortiz et al., 2020)
Distal Basin (Cap Ferret system, Marconi 4)

Figu re 8

Figure 8: In the cross sections published in Ortiz et al., (2020), some parts of the interpretation are of higher resolution than the resolution of the calculations in this paper (i.e. Palaeocene-Eocene, Oligocene, Miocene, Pliocene-Pleistocene). For example, the figure 5 in Ortiz et al., (2020) shows several high resolutions surfaces (thanks to orbitostratigraphy) at 32.2, 32.0, 31.3, 29.4, 27.1, 26.4, 25.2, 24.5, 24.4 Ma for the Oligocene period. This resolution on different parts of the cross section allows us to make a precise quantification shown in the figure. This figure is a compilation of the percentage of 2D area normalized to their duration thanks to high resolution timeline on different cross section published in Ortiz et al., (2020)